AD-A082 567 ITT GILFILLAN VAN NUYS CA F/G 17/9
COMMUTATING FEED ASSEMBLY.(U)
DEC 79 R WOLFSON F19628-79-C-0034
UNCLASSIFIED RADC -TR-79-303 NL

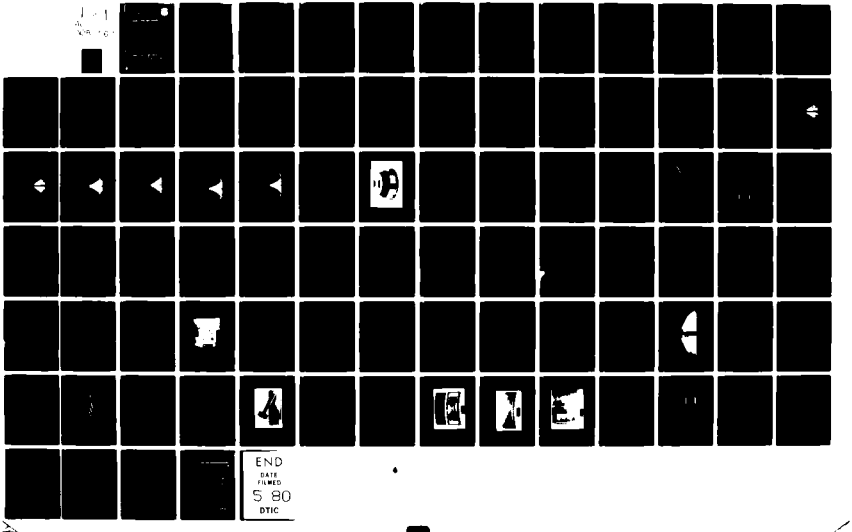

END
DATE FILMED
5 80
DTIC

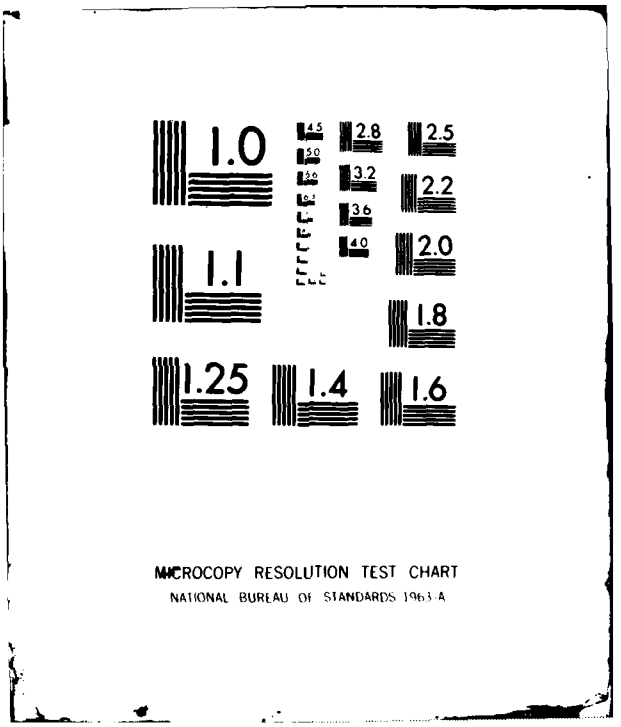
1.0
1.1
1.25
1.4
1.6
1.8
2.0
2.2
2.5
2.8
3.2
3.6
4.0
4.5
5.0
5.6
6.3
MICROCOPY RESOLUTION TEST CHART
NATIONAL BUREAU OF STANDARDS 1963-A

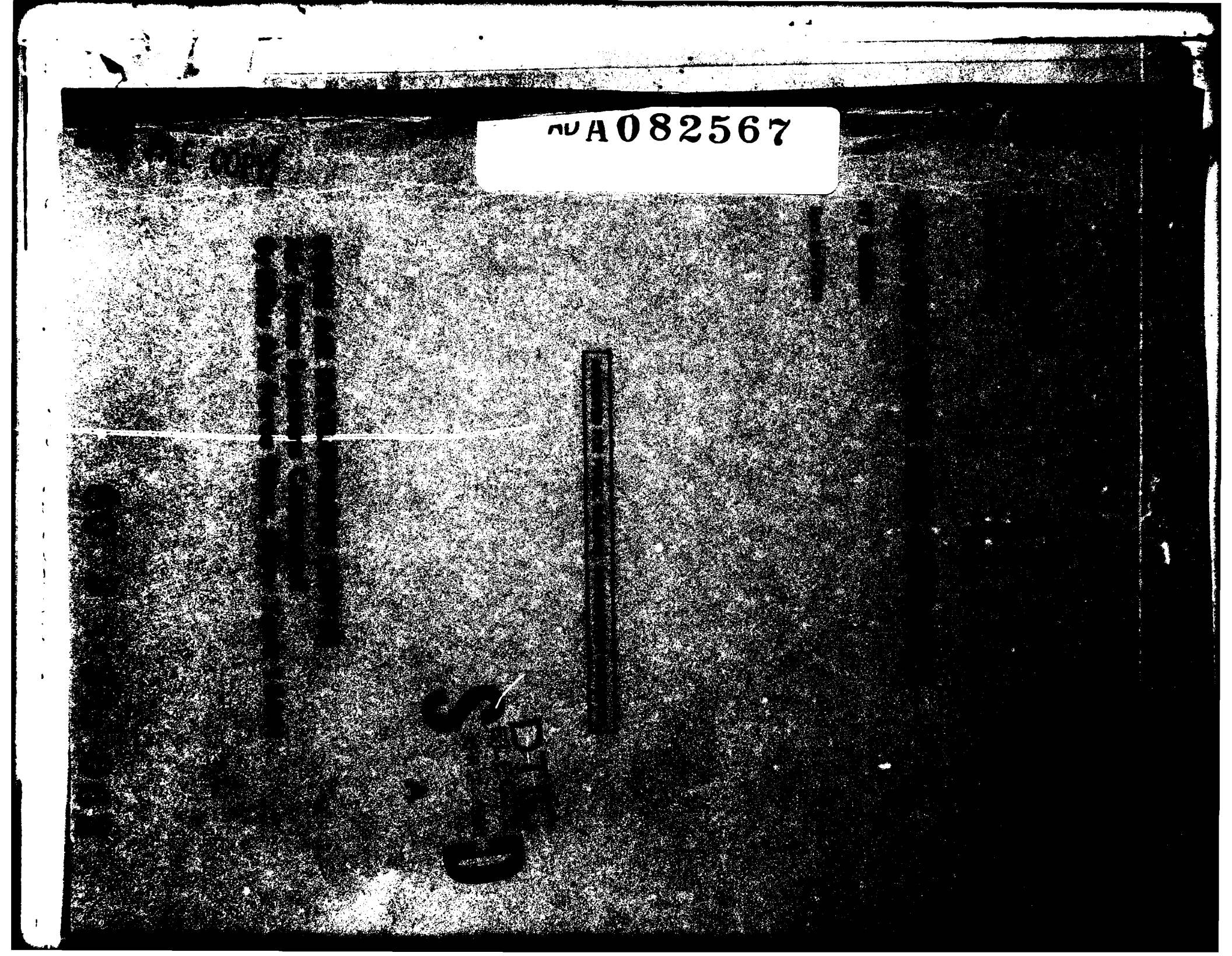
AD A082567

[redacted]

[redacted]
Project Engineer

Approved:

KELAN C. SCHULZ
Chief, Electromagnetic Sciences Division

FOR THE COMMANDER:

JOHN P. HUNT
Acting Chief, Plans Office

If your address has changed, or if you wish to be removed from the mailing list, or if the addressee is no longer employed by your organization, please notify RADC (EMCP), Hanscom AFB, MA 01731. This will assist us in maintaining a current mailing list.

Do not return this copy. Retain or destroy.

TABLE OF CONTENTS

Section

LIST OF ILLUSTRATIONS

LIST OF TABLES

PREFACE

This Interim Report covers the activities conducted during the first seven months of the twelve month effort of the Commutating Feed Assembly, Contract No. F19628-79-C-0034. The development to date of a low-inertia commutating feed for azimuth steering the beam of a circular array ~~is described~~. In addition to superior electrical performance over that of an electronic system, the commutator offers improvements in reliability and life-cycle cost (LCC). It can be accessibly located where maintenance actions are more easily carried out than in an electronically-scanned system or a conventional rotating antenna. Non-contacting loop couplers achieve low-loss transfer and distribution of RF energy, with precise control of amplitude and phase that is needed to realize low sidelobe levels. This method of coupling is preferable to the capacitive coupling used in existing electromechanical commutating feeds, where illumination flutter results in unacceptable MTI performance. To obtain multiple beam groups in elevation, two or more commutators may be stacked on a common drive shaft.

SECTION 1

INTRODUCTION

An electronically scanned circular array antenna is advantageous for applications where 360-degree azimuth scan is required, and where the characteristics of the beam must remain unchanged for every azimuth angle. Electronically scanning a set of three or more planar phased arrays can provide the required 360 degrees of coverage, but results in beam distortion as the angle varies. Mechanically rotating antennas provide the required beam characteristics but usually do not have the required data rate.

Existing all-electronic circular arrays also have disadvantages. In a practical configuration, they require many active subassemblies with an unacceptably large amount of loss, and they require frequent maintenance. In addition, variations in subassembly characteristics due to component differences may cause small variations in the beam characteristics with azimuth scan angle, as well as high sidelobes. The existing Wullenweber electro-mechanical commutating feed has the desirable low drive power and high reliability as it uses a low-inertia mechanically rotating feed. In that device, the power is capacitively coupled from a rotating to a stationary transmission line that connects to the large circular array elements. However, the capacitive coupling used causes unacceptable loss and flutter, or fluctuations in the radiated beam with rotational angle.

Large-scale parallel-plate combiner/dividers have been developed by ITT Gilfillan that make use of a magnetic loop coupler. This device derives its properties from both the waveguide loop coupler and the -3dB quarter-wave directional coupler. In the waveguide version, matched coupling to the dominant mode is obtained by proper quarter-wave transformation of the waveguide impedance to that of the coaxial input. Wide bandwidth is insured by coupling to the fields in a manner that minimizes impedance change, thereby reducing the Q of the network. The use of magnetic loop couplers in a commutating feed provides low RF loss and inertia while limiting flutter to the narrow range of angles where the rotor loops pass over small gaps between adjacent stator loops.

SECTION 2

COMMUTATING FEED ASSEMBLY REQUIREMENTS

The overall objectives are to develop, construct and test a power divider and commutator to feed an electronically rotating 90° sector of an Unattended Radar (UAR) circular array, and to study the costs, reliability and fabrication costs of production versions of the device.

Table 2-1 presents a summary of the requirements for the Commutating Feed Assembly. Significant mechanical requirements include a drive power of below 50 watts and the ability to stack two or more commutators for systems with multiple beams. In addition, the system concept should be readily extendable to a circular array with approximately 200 outputs, with as many as one-third of these excited at one time. Other important considerations are the environmental conditions encountered in the Arctic, as well as the extremely high MTBF required for unattended operation. For high-performance radar operation, low phase and amplitude variations are required for good MTI performance. In addition, electrical contact noise often encountered in electro-mechanical assemblies must be minimized.

TABLE 2-1. COMMUTATING FEED ASSEMBLY REQUIREMENTS

Frequency Band	1.2 to 1.4 MHz
Number of Output Ports	100
Number of Excited Ports	26
Excited Sector	90°
Aperture Illumination	Consistent with -20 dB Sidelobes
VSWR	
Input Port	1.3:1 maximum
Output Ports	1.3:1 maximum
Insertion Loss	1.0 dB maximum
Power Capacity	
Peak	10 kW
Average	500 W
Rotation Rate	15 rpm
Drive Power	50 Watts maximum
Environment	-35°F to $+100^{\circ}$F minimum (as encountered in Arctic)
Reliability	Consistent with Unattended Radar operation
Stacking	2 or more Commutators
Growth	200 Outputs 68 Excited

SECTION 3

TECHNICAL PROBLEMS

Increasing emphasis is being placed on minimizing the total Life Cycle Cost of new radar programs. At the same time, more stringent mission requirements call for increased operational availability, A_o, and reduced repair times. These goals are perhaps best exemplified in the U.S. Air Force SEEK FROST program. This program is examining the replacement of current DEW Line radars with equipments that will operate unattended for extended periods of time of up to one year. Maintenance teams located at centralized maintenance nodes will provide preventive and emergency repair services for these sites. The reduction in the total number of personnel required to operate and maintain the line is expected to reduce significantly O&M costs from that of the existing system.

For unattended operation, it is clear that very high reliablity designs are required. This includes not only the designs of the individual components, but also the fundamental architectures of major subsystems. An additional consideration relating to both operating costs and reliability is the overall system efficiency and power consumption. This becomes especially important due to the rapidly escalating costs of energy, and to the costs and difficulties associated with replenishing the supply of energy at isolated sites.

One of several antenna concepts being considered for systems such as the UAR is a circular array, shown in Figure 3-1. The principal motivations for such an approach over a conventional rotating antenna are reduced drive power, improved reliability, and availability of simplified maintenance. Over the past decade, numerous purely electronic scan concepts for circular arrays have been developed. All of these approaches have been plagued by high loss and poor reliability due to the large number of components in series, and poor sidelobe performance due to large amplitude and phase errors.

To address these problems, the Department of the Air Force, Electronic Systems Division, has funded ITT Gilfillan to develop, construct and evaluate a Commutating Feed Assembly for steering the beam of a circular array. The advantages of such an approach are simplicity, low cost, and low drive power. Properly designed, such a commutator offers superior electrical performance over an electronic system and significant improvements in reliability and LCC.

3.1 System Design

3.1.1 Radius of Circular Array

The specifications given for the model circular array include 100 columns of vertical dipole radiators with an inter-element spacing of 0.62λ at the design frequency of 1.3 GHz. The diameter of such an array is nominally 180 inches. The chosen number of array elements is one-half that required for a full-sized antenna with the same inter-element spacing.

Azimuth patterns were computed for several circular array designs using two different design illumination functions, and several diameters for a fixed total number of array columns. The illumination functions chosen are -25dB, $\bar{N} = 4$ Taylor and -29dB, $\bar{N} = 4$ Taylor. Array diameters of 180, 160 and 135 inches are used for the model array, and 360, 320 and 270 inches for the full-sized array. The illumination sector used is 90 degrees for all cases; in addition, a 120-sector is considered for the full-sized array.

The patterns shown in Figures 3-2 through 3-7, are computed at the upper frequency end of the band, 1.4 GHz. As expected, the designs with the largest inter-column spacing, 0.67 wavelengths at this frequency, show high grating lobes which in some cases do not meet the -20 dB sidelobe level requirement. The exact level of the grating lobe is influenced appreciably by the azimuth pattern of an individual column. All the cases shown assume a cosine element power pattern.

As the primary purpose of this development is to demonstrate the feasibility of a low-inertia commutating feed, work will proceed on the basis of a 0.62λ inter-element spacing at 1.3 GHz. However, to realize the potential low-sidelobe performance of which this commutator feed concept is capable, further analysis of the circular array antenna system is indicated.

3.1.2 Design Illumination

Three types of illumination function were considered for this application: Taylor, Chebyshev, and a modified (sin u)/u. The Taylor illumination produces a determined number of near-in sidelobe pairs at the design level, after which the sidelobe structure gradually decays to the level established by random errors. For most applications with moderate sidelobe-level requirements, this function is preferred because it results in the best compromise between sidelobe level and aperture efficiency, and in practice the element-coupling values are readily achievable. The Chebyshev illumination results in all sidelobes at essentially the same level; very low first sidelobes can be obtained at the expense of foregoing further reduction in the level of far-out sidelobes. This illumination function is the most efficient of the three types mentioned, but can be difficult to realize because of the precise amplitude control required at the edge elements. The (sin u)/u function, which is the least efficient of these, gives a gradual reduction in sidelobe level after the first pair until the random-error level is reached.

As shown in the computed patterns of Figure 3-2, a -25dB, $\bar{N}$ = 4 Taylor distribution readily fulfills the sidelobe level specification of -20dB with adequate margin, except for the grating lobes at 1.4 GHz in the 180-inch diameter circular array. However, a -29dB, $\bar{N}$ = 4 Taylor distribution will be used for the model Commutating Feed Assembly in order to demonstrate the potential low-sidelobe performance more convincingly. The penalty in aperture efficiency for chosing a -29dB rather than -25dB Taylor excitation is about 0.25dB.

3.1.3 Elevation Scan Angle for Zero Phase Error

In order to obtain a planar wavefront from a circular array of radiating elements, it is necessary to compensate for unequal pathlengths that occur in space due to curvature of the array. The geometry for this situation is illustrated in Figure 3-8. The differential pathlengths relative to the edge elements that are required for a planar wavefront are given by the equation

$$\Delta \ell_n = \frac{R\,(\cos\phi_n - \cos\phi_{max})\cos\theta}{\sqrt{\epsilon_r}}$$

where:

R = radius of circular array,
ϕ_{max} = one-half of sector angle,
ϕ_n = angle of n^{th} element relative to center of sector,
θ = desired elevation scan angle for zero phase error, and
ϵ_r = relative dielectric constant of stripline feed.

Note that the differential pathlengths, $\Delta \ell_n$, required for a planar wavefront are a function of elevation scan angle, θ. Thus, the circular array can be compensated exactly only at one preselected value of elevation scan angle. A value of 15 degrees is assumed, as this angle is the maximum value of θ for which there is essentially no degradation in beamwidth and sidelobe performance at the horizon. As $\Delta \ell_n$ is independent of frequency, this configuration is inherently broadband.

3.1.4 RF Loss Budget

Total pathlength in stripline between input and rotor loop averages about 60 inches; thus, the insertion loss of the stripline feed network is about 0.7dB. The overall Commutating Feed Assembly loss budget is given in Table 3-1.

TABLE 3-1. LOSS BUDGET OF COMMUTATING FEED ASSEMBLY

Component	Loss
Rotary Joint	0.2
Stripline Feed	0.7
Loop Couplers (including mismatches)	0.2
Coax and Connectors	0.1
Total Loss	1.2 dB

3.2 Rotator Pedestal Assembly

3.2.1 Drive Train

The function of the drive train is to rotate the stripline feed assembly at a constant rate of 15 rpm with high efficiency and high reliability. Although both an ac motor and a dc torque motor were considered for this application, the latter type was chosen for the following reasons:

(a) A dc torque motor contains only one moving part, the rotor, whereas an ac motor must also have a gear-reduction train that requires lubrication. As a consequence of having fewer moving parts, the dc torque motor is more reliable.

(b) The bearing life of the dc torque motor is longer for two reasons. First, the dc torque motor selected has only two bearings, both large, whereas the ac motor and associated gear train have several bearings, all small. Large bearings result in less loading, which is a significant factor in bearing life. A second important key to bearing life is shaft speed, which is at least two orders of magnitude less for the dc torque motor than for the ac motor.

(c) The dc torque motor provides high starting torque. This feature is particularly important for failsafe starting of the Commutating Feed Assembly in sub-zero climate during periods of routine maintenance.

(d) The dc torque motor is more efficient than an ac motor, primarily because the need for a gear-reduction train is eliminated.

Figure 3-9 is a photograph of an existing rotator pedestal assembly. The unit selected for this program uses the same basic housing casting, with modifications to the internal parts. The motor is a 7 ft-lb dc torque motor. An access door could be provided in the side of the pedestal in order to facilitate maintenance. This would eliminate the need to disassemble or remove the commutator for replacement of motor brushes.

Figure 3-10 shows the estimated drive power required both for startup and for continuous rotation at 15 rpm as a function of stripline rotor diameter. It is seen that for both conditions, considerably less than the specified 50 watts maximum drive power is necessary.

Figure 3-11 similarly shows the estimated drive power required for a number of 3-foot diameter stripline rotors stacked on a common shaft. It is seen that up to five commutators can be driven within the 50-watt drive power limitation.

3.2.2 Support Structure

The support structure of the Commutating Feed Assembly is shown in Figure 3-12. Brace supports are bolted between the pedestal drive assembly housing and the stripline feed housing, to form a rigid, lightweight structure.

3.3 Annular Rotary Coupler

Power is fed to the rotating feed network through a rotary joint from the input line. In order to stack two or more commutators on a common drive shaft, an annular rotary coupler with access hole through the center is required. A trade off exists between annular rotary coupler insertion loss and VSWR on one hand, and hole diameter on the other. Typical parameters for two different size units over the 1.2 to 1.4 GHz frequency band are given in Table 3-2.

TABLE 3-2. TYPICAL PARAMETERS FOR ANNULAR ROTARY COUPLERS

Hole Diameter, Inches	Insertion Loss, dB	VSWR
0.406	0.2	1.20:1
1.000	0.5	1.50:1

For the experimental model commutator, an annular rotary coupler with a 13/32-inch diameter hole was selected in order to take advantage of the superior electrical characteristics. This allows the use of a 3/8-inch diameter drive shaft, which is

adequate for a single or two stacked commutators. For multiple stacked units, excessive tortional strain of this size shaft may result in loss of synchronization among the several commutators. Further analysis is needed in order to assess the magnitude of the problem, and to determine the optimum annular rotary coupler configuration for hole diameter and electrical performance.

3.4 Stripline Feed Network

Figure 3-13 shows a schematic of the rotating stripline feed network. A diameter of approximately three feet is required to allow sufficient space for the amplitude distribution networks and delay lines that provide the circular-array phase compensation. TEM delay lines produce the correct phase independent of frequency. The amplitude distribution networks consist of stripline couplers that provide the proper cylindrical-array illumination amplitude for -30 dB sidelobes.

Several types of array feed networks were considered for this application. Parallel or corporate-feed approaches were rejected because of their high sensitivity to coupling errors, difficulty in realizing the required illumination with a reasonable range of coupling values, and excessive size. Center-fed equal-pathlength (before phase compensation) series array feeds were selected for their low loss, wide bandwidth, relative insensitivity to coupling errors, and compact form factor.

3.4.1 Range of Coupling Values vs. Percent Power into Load

A trade-off exists in the design of a series feed network between the range of element coupling factors and the amount of power dissipated in the main-line load termination. This is illustrated in Figure 3-14 for a 13-element series feed with -29 dB, $\bar{N} = 4$ Taylor illumination. It can be seen that with no power into the end load, a wide range of coupling factors is required: 0 dB to -7.47 dB. With 3% power into the end load, which represents an additional insertion loss penalty of only 0.13 dB, a more viable range of design coupling factors is obtained: -5.56 dB

to -7.60 dB. The use of nearly equal coupling factors also gives better element-to-element amplitude and phase tracking, so that array performance at the operating band edges is only minimally affected.

3.4.2 Coupler Configuration Trade-Off

In order to select the best type stripline coupler for this application, a trade-off study of key parameters was made for several commonly used coupler configurations. A nominal coupling factor of -6 dB was assumed, with performance considered over the 1.2 to 1.4 GHz radar band alone, as well as the extended band of 1.03 to 1.4 GHz to include IFF. The results of this trade-off study are summarized in Table 3-3. The single-section branchline coupler was rejected due to high VSWR, low isolation, and excessive phase runout. The hybrid ring coupler is acceptable electrically, but is too large, with the ports awkwardly located for a series feed. The compensated in-line divider has excellent electrical characteristics, but is long, and requires an internal isolating resistor that is often not readily accessible. Best electrical performance is obtained with the two types of quarter-wave coupler. Where coupling tighter than -10 dB is needed, the $\lambda/4$ sidewall coupler becomes impractical to reproduce because of the small, accurate, etched gap required. This problem is avoided with the $\lambda/4$ overlap coupler, where the through and coupled lines are etched on opposite sides of a thin dielectric board. This type of coupler requires a 3-layer construction with accurate front-to-backside registration.

3.4.3 Choice of Stripline Material

Four stripline configurations were considered for this application: air-strip, foam dielectric, honeycomb, and the conventional solid-dielectric sandwich type. Of these, air-strip has the least insertion loss per unit length, with foam, honeycomb and then solid dielectric following.

TABLE 3-3. COMPARISON OF -6 dB STRIPLINE COUPLERS

PARAMETER	BRANCHLINE COUPLER	HYBRID RING COUPLER	COMPENSATED IN-LINE DIVIDER	λ/4 SIDEWALL COUPLER	λ/4 OVERLAP COUPLER	REQUIRED VALUE
Operating Band						
Required (GHz)	1.2 - 1.4	1.2 - 1.4	1.2 - 1.4	1.2 - 1.4	1.2 - 1.4	1.2 - 1.4
Other (GHz)	1.03 - 1.09	1.03 - 1.09	1.03 - 1.09	1.03 - 1.09	1.03 - 1.09	
Board Size (ϵ_r = 2.5)	1.7" X 1.7"	3.0" X 3.0"	0.8" X 4.5"	0.5" X 1.7"	0.4" X 1.7"	Approx. 2" X 2" max.
Coupling Values						
Required (dB)						-5 to -8
Practical (dB)	-3 to -9	-3 to -9	-3 to -10	Weaker than -10	-3 to -30	
Coupling Flatness (dB)	0.05 0.25	0.20 0.60	0.10 0.20	0.02 0.08	0.02 0.08	<0.2/0.6*
VSWR	1.12:1 1.26:1	1.06:1 1.18:1	1.05:1 1.12:1	<1.05:1	<1.05:1	<1.05:1/1.20:1*
Isolation (dB)	14 8	27 20	32 25	>30	>30	>25/16*
Phase Runout	14° 19°	2° 4°	≤0° ≤0°	≤0°	≤0°	<2°/5°*
Special Features	Thru & coupled ports are adjacent	Thru & coupled ports are separated by input port	Requires internal isolating resistor	Requires small gap for tighter than -10 dB coupling	Requires 3-layer construction with accurate registration	
Estimated relative production cost	0.7	0.6	0.5	0.6	1.0	

1878-16

*Values given are for sidelobe levels of -30dB and -20 dB respectively; required SLL is -20 dB.

A solid Teflon-fiberglass dielectric medium was finally selected for moderate cost, good mechanical properties, low-loss characteristics, and reduction of wavelength in the medium, with correspondingly smaller size. A summary of the stripline material properties is given in Table 3-4.

TABLE 3-4. PROPERTIES OF TEFLON-FIBERGLASS

Dielectric Constant	2.5
Loss Tangent	0.0012
Usable Temperature Range	$-40^{\circ}C$ to $+200^{\circ}C$
Tensile Strength	15 kg/mm^2
Flexural Strength	10 kg/mm^2
Thermal Conductivity	2.6×10^{-4} $cal/sec/cm^2/^{\circ}C/cm$
Coefficient of Thermal Expansion	10×10^{-6} $(cm/cm)/^{\circ}C$
Thickness range available	0.20 to 0.125 inches
Specific Gravity	2.2

Because of the 3-layer construction required for overlap couplers, the stripline configuration shown in Figure 3-15 was chosen. A total ground-plane spacing of 0.270 inch provides a reasonable compromise between insertion loss, 0.0114 dB/inch, and line width, 0.190 inch for 50 ohms.

The center-board thickness of 0.020 inch represents a trade-off between two undesirable effects. As the center board becomes thinner, the coupling factor accuracy becomes increasingly more sensitive to the degree of overlap in the couplers. For example, a $\pm$ 0.001 inch error in overlap results in a $\pm$ 0.2 dB error in coupling factor for 0.020-inch thick material, and $\pm$ 0.3 dB error for 0.010-inch thick material. On the other hand, if the center board is made thick with respect to the outer dielectric sheets, the center conductor does not lie on the centerline between ground planes. If this unbalance is too great, serious moding problems can result.

½-ounce copper was chosen for cladding the center board rather than the usual 1-ounce or 2-ounce copper. This provides greater etched-line definition in the critical overlap region, but does not appreciably affect insertion loss or average power-handling capability.

3.4.4 Delay Line Phase Compensation

The feed network uses delay lines of appropriate length, as shown in Figure 3-16, to provide the exact phase correction required at each element. For an antenna 180 inches in diameter with an illumination sector of 90^{o}, the pathlength in dielectric to the center element must be 16.077 inches longer than to the edge element. The additional insertion loss of as much as 0.18 dB due to the differential pathlengths must be considered in determining the coupling factors of the series line feed.

3.4.5 Phase Trimmers

In order to realize first sidelobes of -30 dB, the element-to-element phase error must be held to about 2^{o} or less. However, accumulated phase errors in a stripline package of this kind could run as large as 10^{o} due to various tolerances and uncontrolled factors. Some of these sources of error are the thickness and dielectric constant of the boards, etched line widths, line lengths, miters, impedance mismatches, solder connections and connectors. Double-stub phase trimmers with approximately 15^{o} of adjustment range, similar to Figure 3-17, will be placed in each of the 26 coupled lines so that accumulated phase errors in the rotating stripline feed assembly can be corrected to an acceptably low value.

3.5 Loop Couplers

Operation of the magnetic loop couplers can be explained by referring to Figure 3-18. The device shown schematically on the left is a conventional quarter-wavelength directional coupler in TEM transmission line. If the normal thru and coupled ports are short-circuited as shown on the right, and the line impedances and coupling factor are properly adjusted, all of the input power, minus losses, can be routed to the indicated port. The 0-dB coupler exhibits many of the fine performance traits of the conventional $\lambda/4$ coupler, namely low insertion and wideband operation.

3.5.1 Loop-Coupling Region

A plan view of the loop-coupling region of the Commutating Feed Assembly is shown in Figure 3-19. The coupling performance is expected to vary somewhat as the rotor loops pass over the stator loops. These variations are minimized in magnitude and duration by using magnetic coupling with narrow rotor loops and much wider stator loops. Of course, during the interval when the rotor loop is over the gap region between adjacent stator loops, the effect is most noticeable. This situation can be avoided either by staggering the relative location of rotor and stator loops, or by transmitting and receiving only when the loops are well engaged.

Rotor loop fabrication and assembly can be improved significantly by etching them directly on the stripline circuit board. This solves the problem of how to attach the rotor loops both mechanically and electrically to the stripline feed network in an inexpensive and reliable fashion.

3.5.2 RF Chokes

Proper operation of the magnetic loop couplers requires that the quarter-wavelength loops are terminated in a reliable, low-loss RF short. This is easily accomplished for the stator loops by means of the aluminum shorting bar that is used to support the grounded end of each loop. The problem is more complicated for the rotor loops, which continually move relative to the commutator housing. A contacting short is undesirable from the standpoint of loss, reliability, wear, and the generation of electrical contact noise. Therefore, RF chokes of the standard double quarter-wavelength design are used to provide non-contacting RF shorts for the rotor loops. Two RF chokes are required: one in the lower housing surface that produces an RF short in the plane where the stripline ground planes end and the rotor coupling loop begins; and a second RF choke in the upper housing surface that produces an RF short in the plane of the grounded end of the rotor loop.

Each choke cavity can be made by machining an annular groove in the housing surface, and then using a washer-shaped ring to form the folded quarter-wavelength sections.

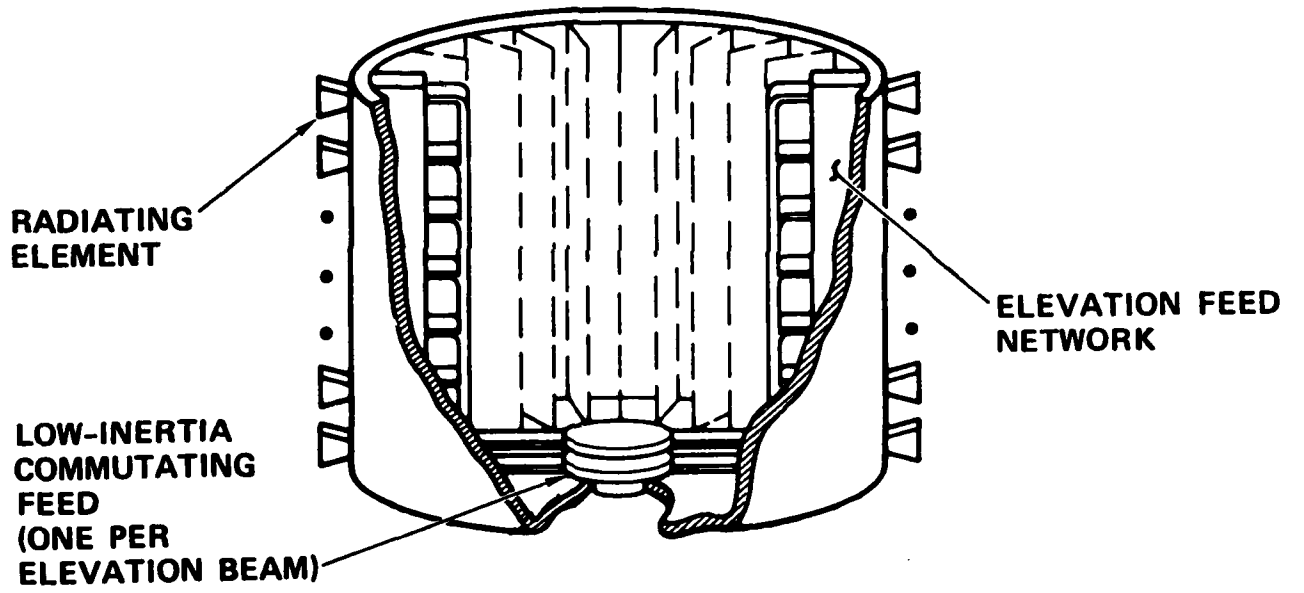

Figure 3-1. Circular Array Antenna Concept Using Low-Inertia Commutating Feed

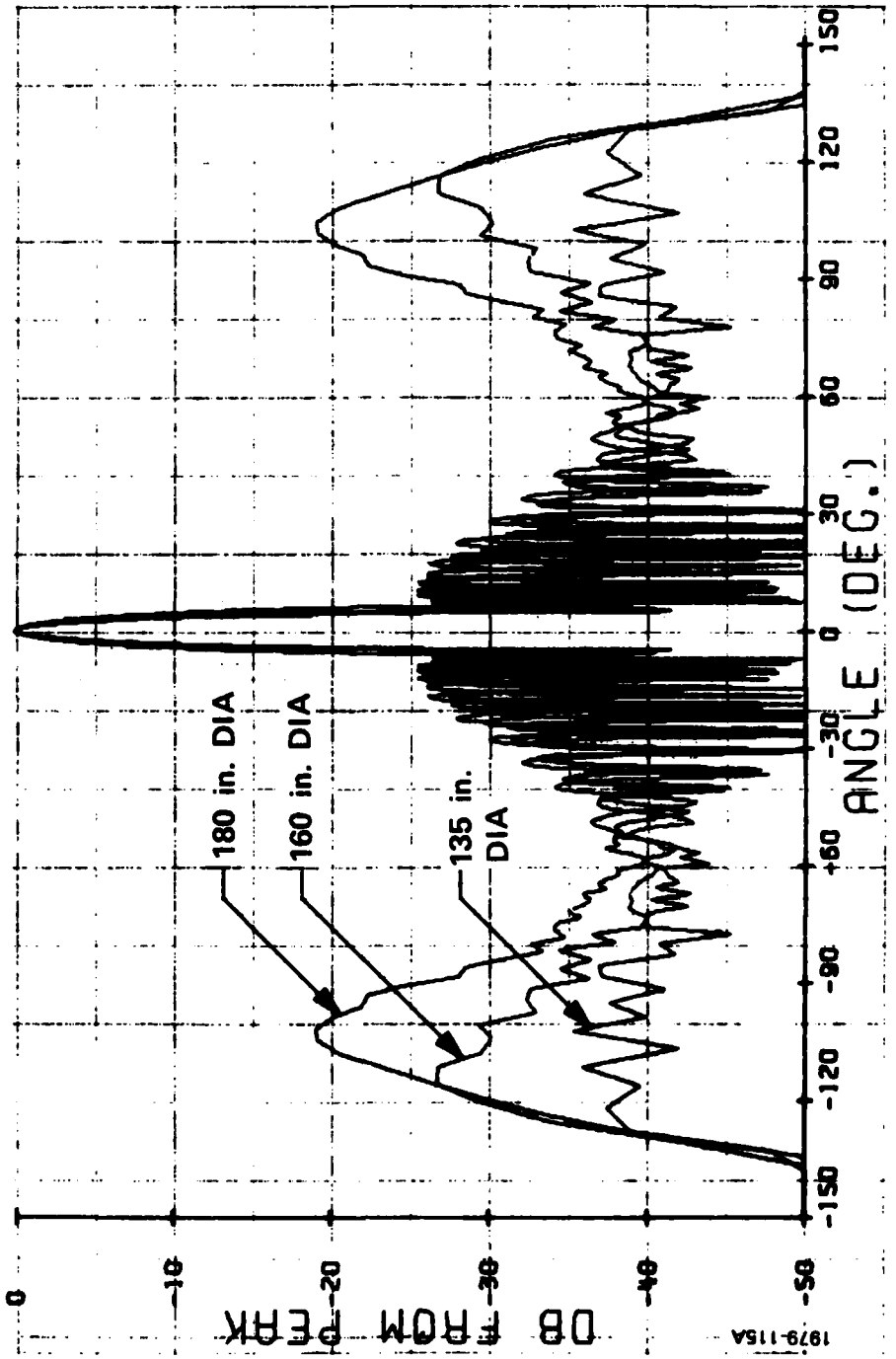

Figure 3-2. Computed Azimuth Patterns: 100 Elements, 90° Sector, -25 dB Taylor Illumination

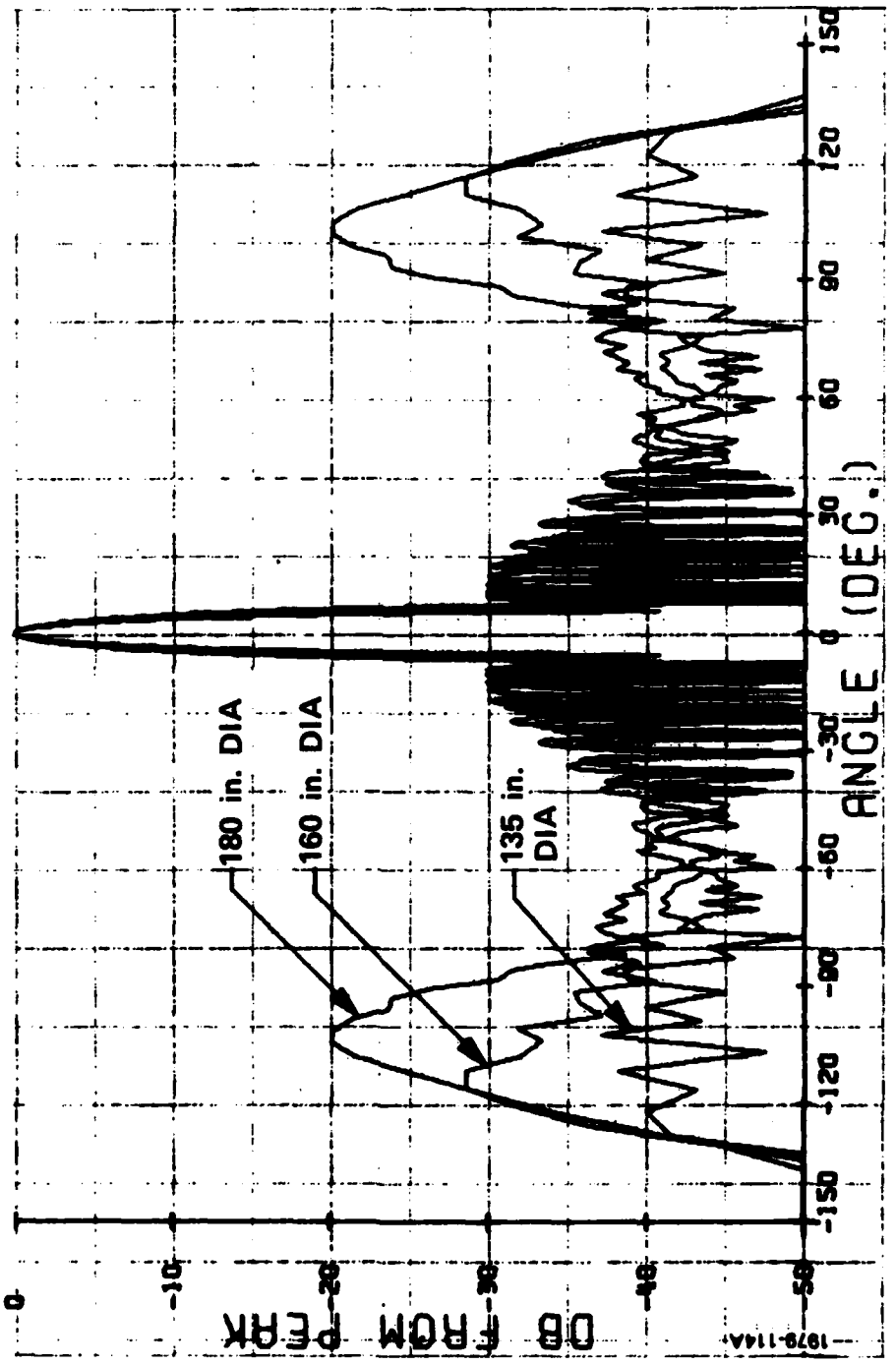

Figure 3-3. Computed Azimuth Patterns: 100 Elements, 90° Sector, -29 dB Taylor Illumination

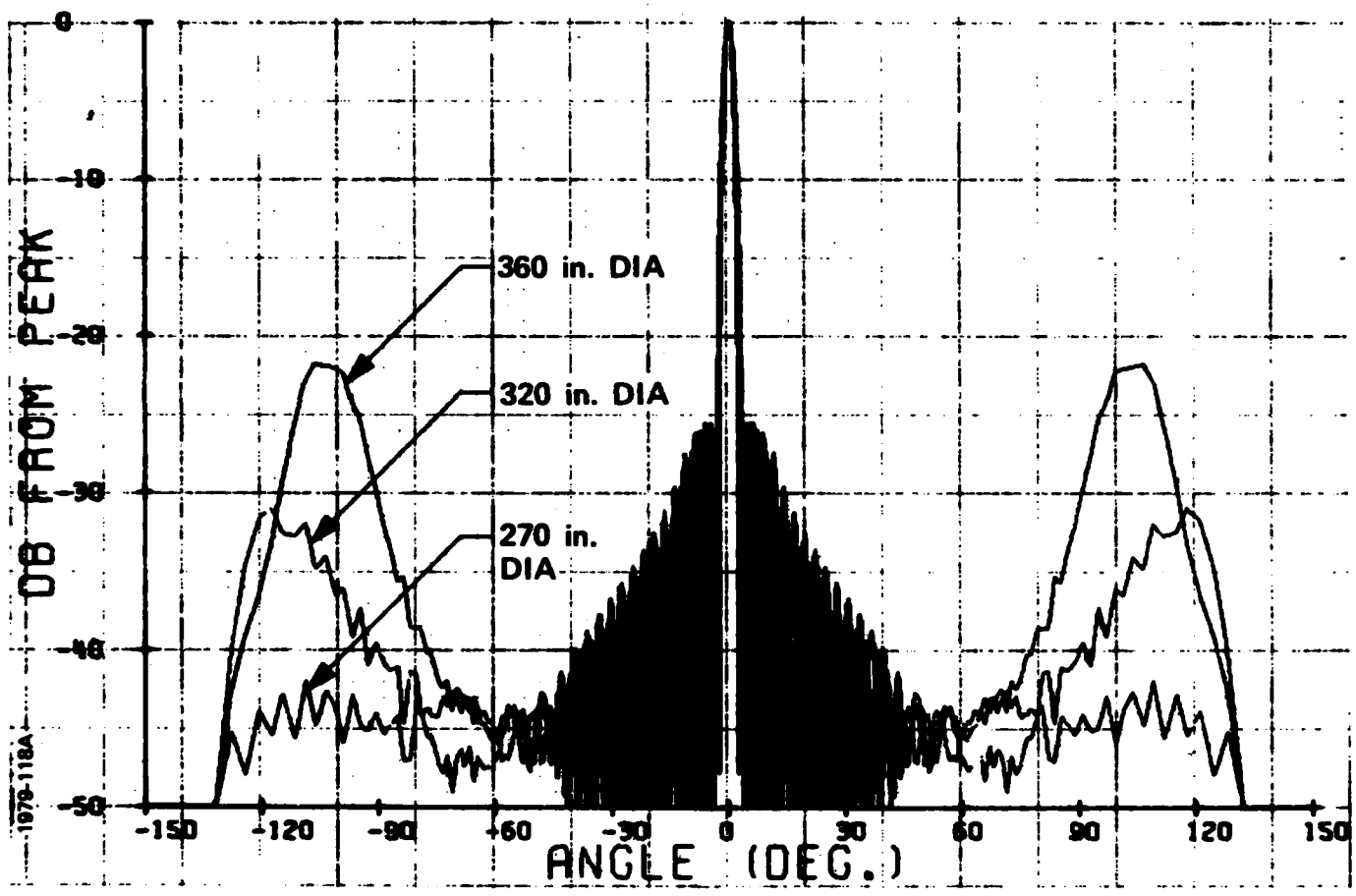

Figure 3-4. Computed Azimuth Patterns: 200 Elements, 90° Sector, -25 dB Taylor Illumination

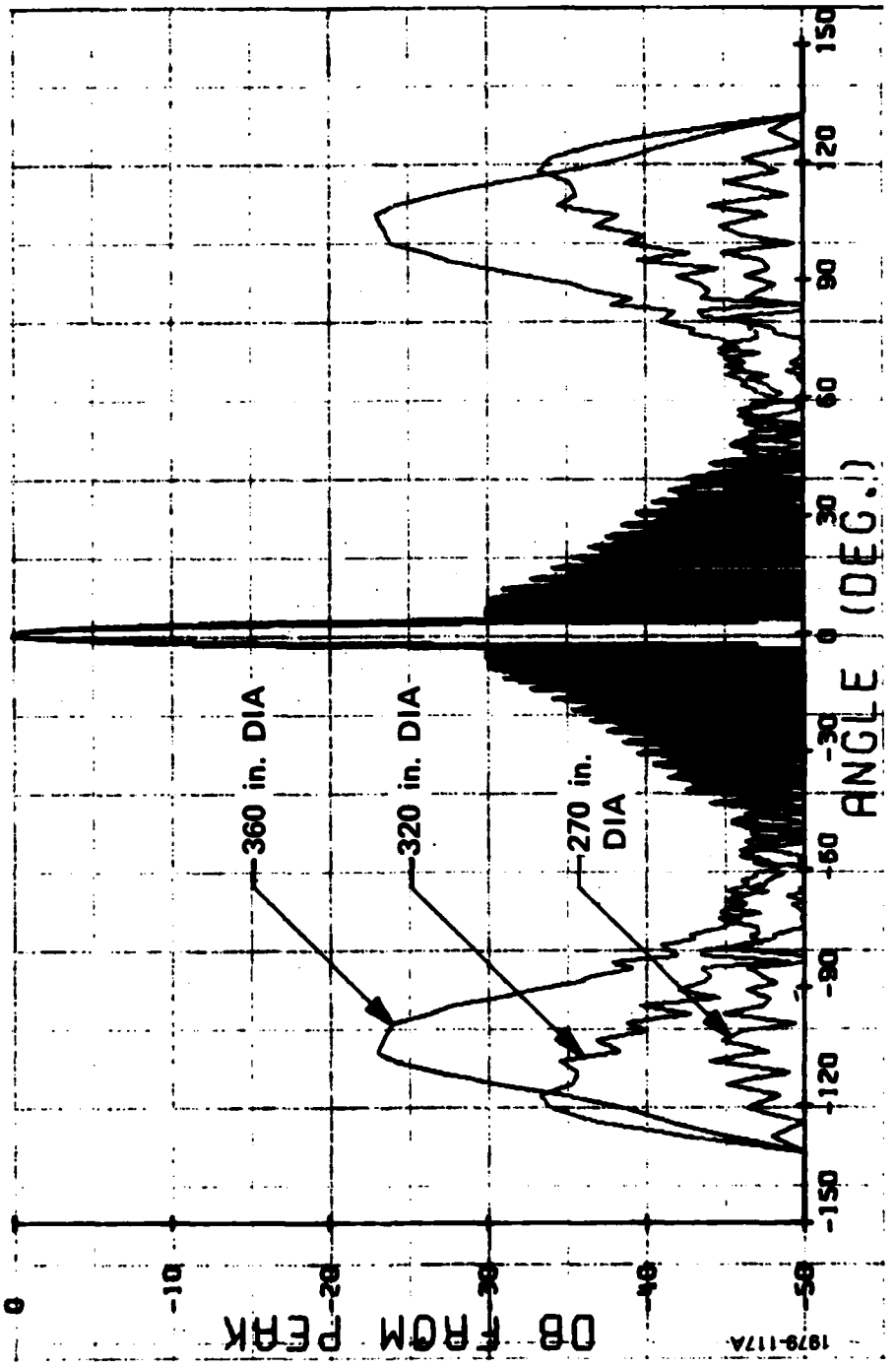

Figure 3-5. Computed Azimuth Patterns: 200 Elements, 90° Sector, -29 dB Taylor Illumination

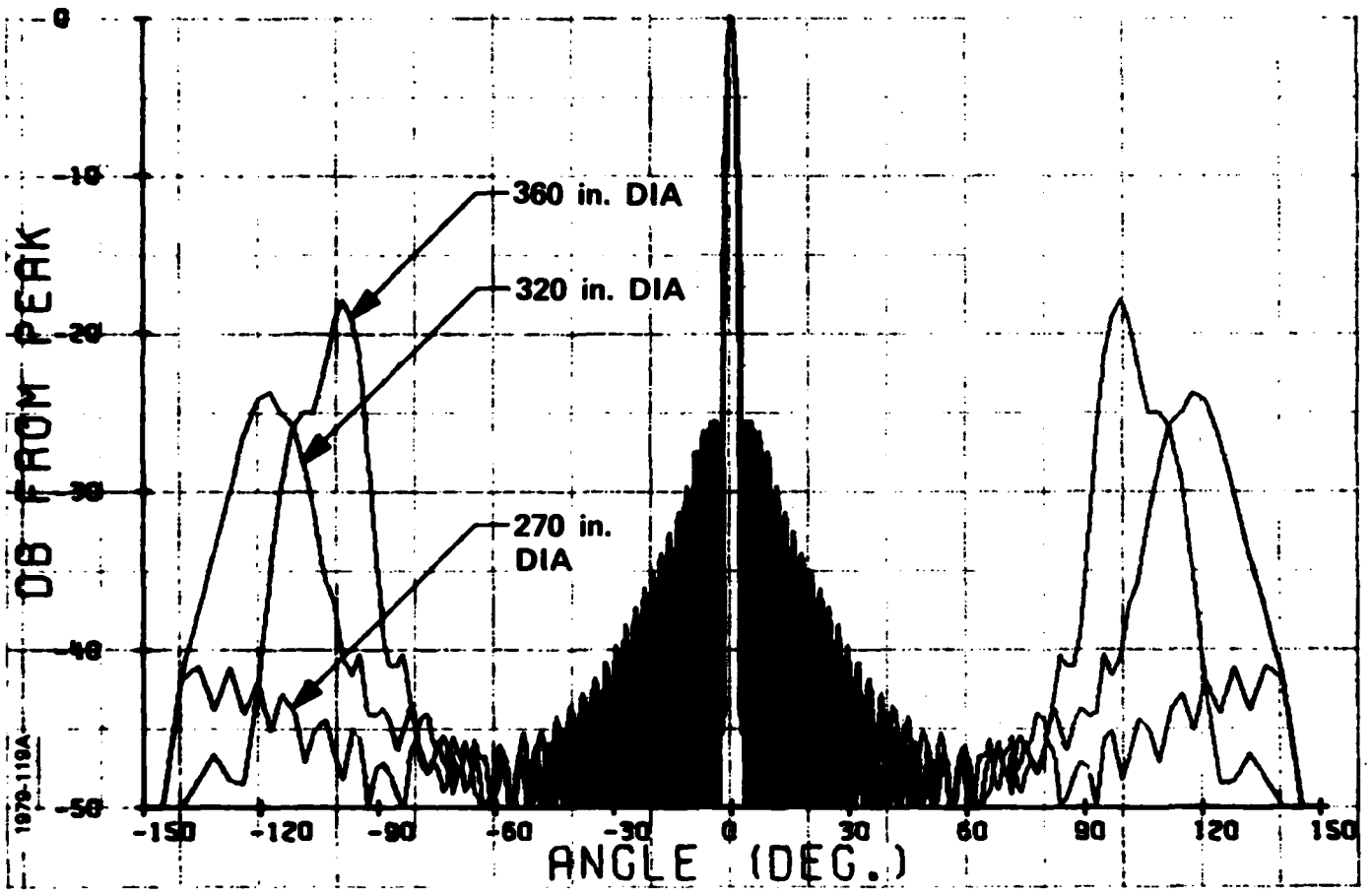

Figure 3-6. Computed Azimuth Patterns: 200 Elements, 120° Sector, -25 dB Taylor Illumination

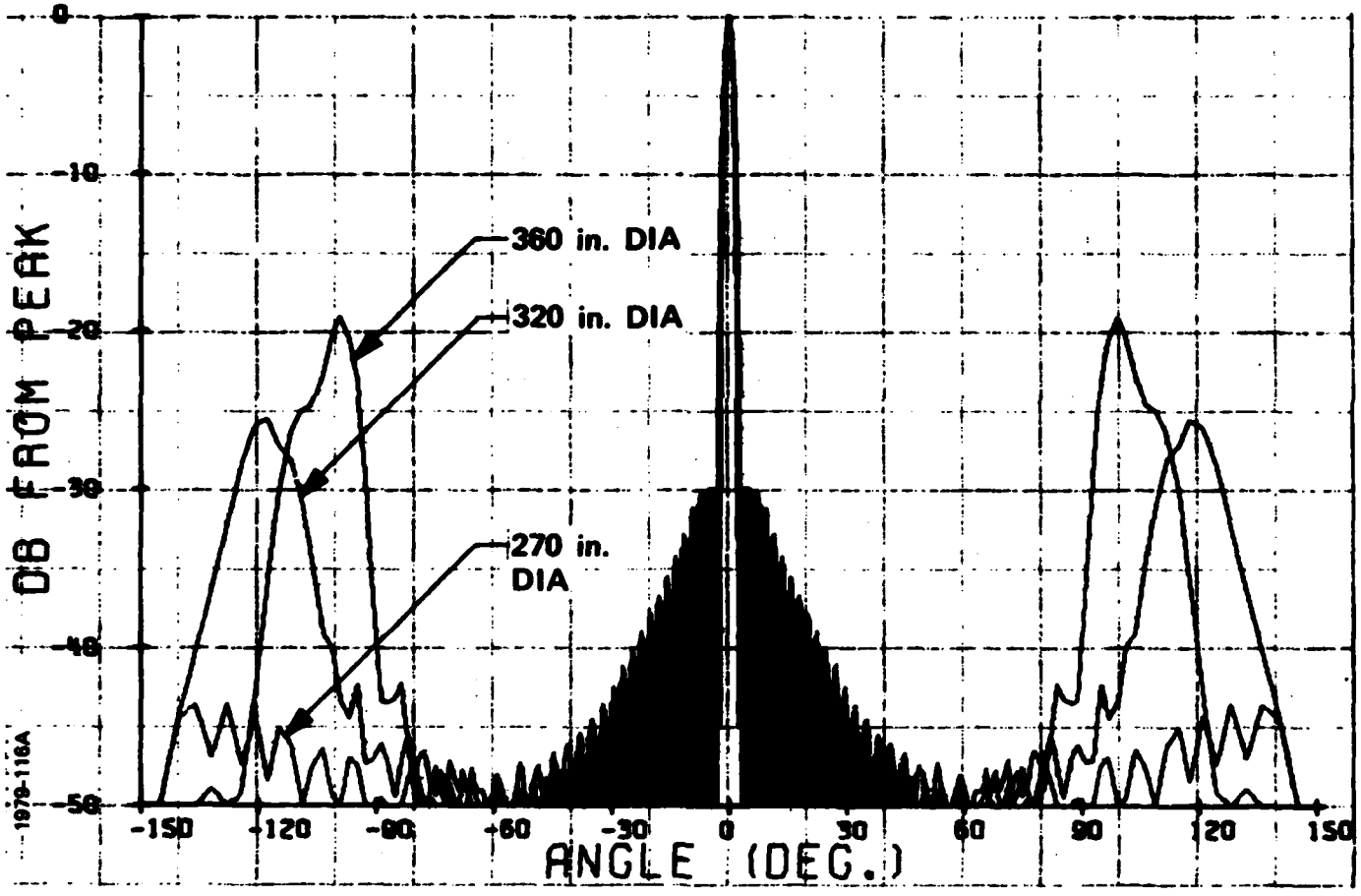

Figure 3-7. Computed Azimuth Patterns: 200 Elements, 120° Sector, -29 dB Taylor Illumination

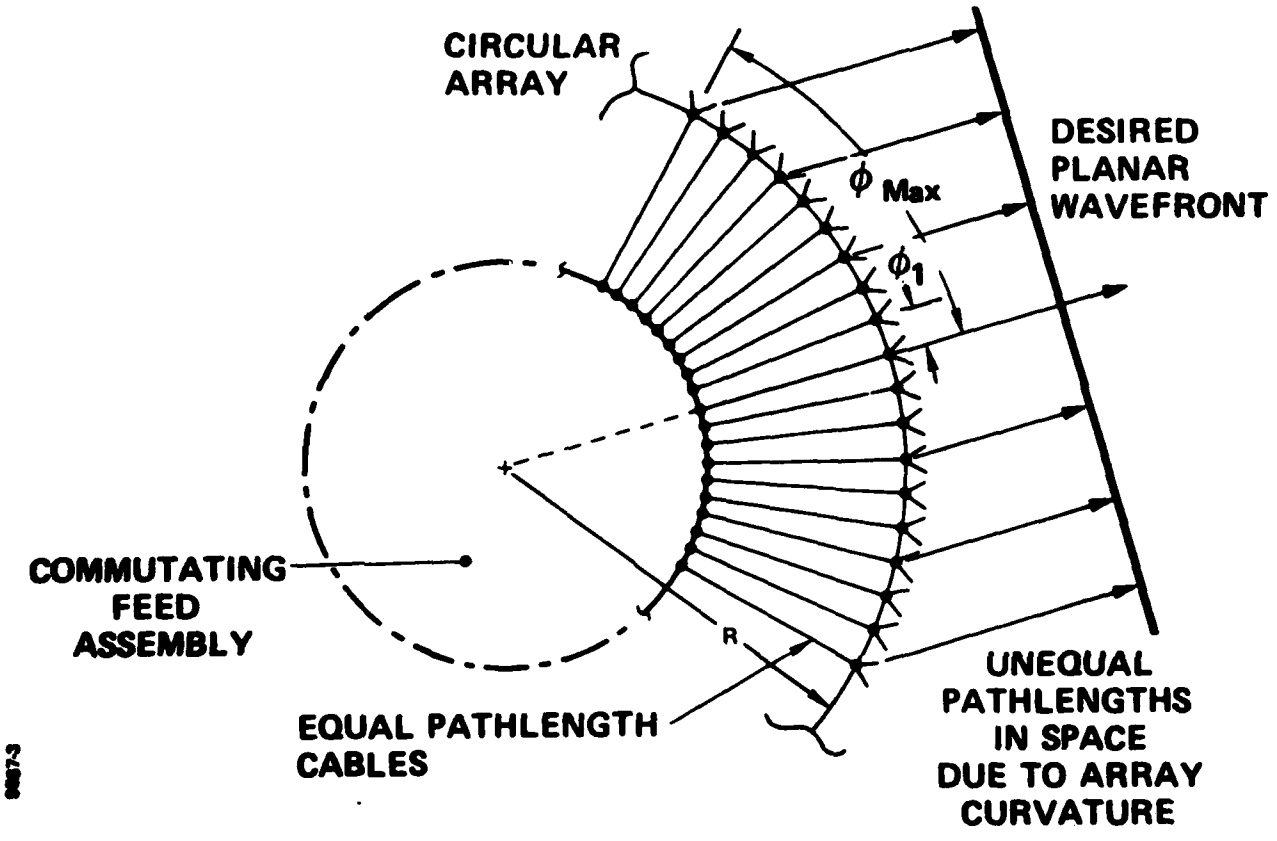

Figure 3-8. Pathlength Variations in Circular Array

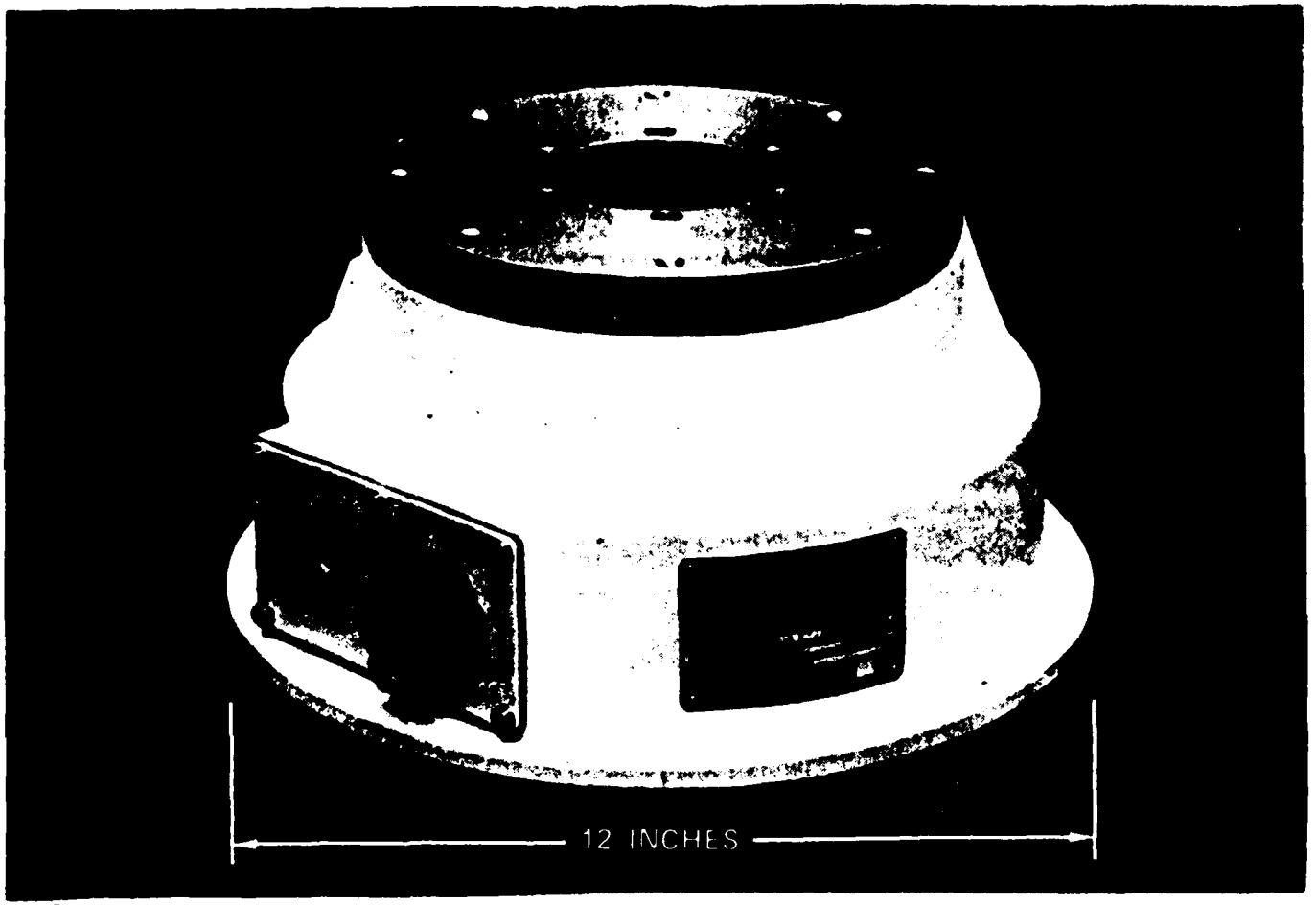

9001-2

FIGURE 3-9. ROTATOR PEDESTAL ASSEMBLY

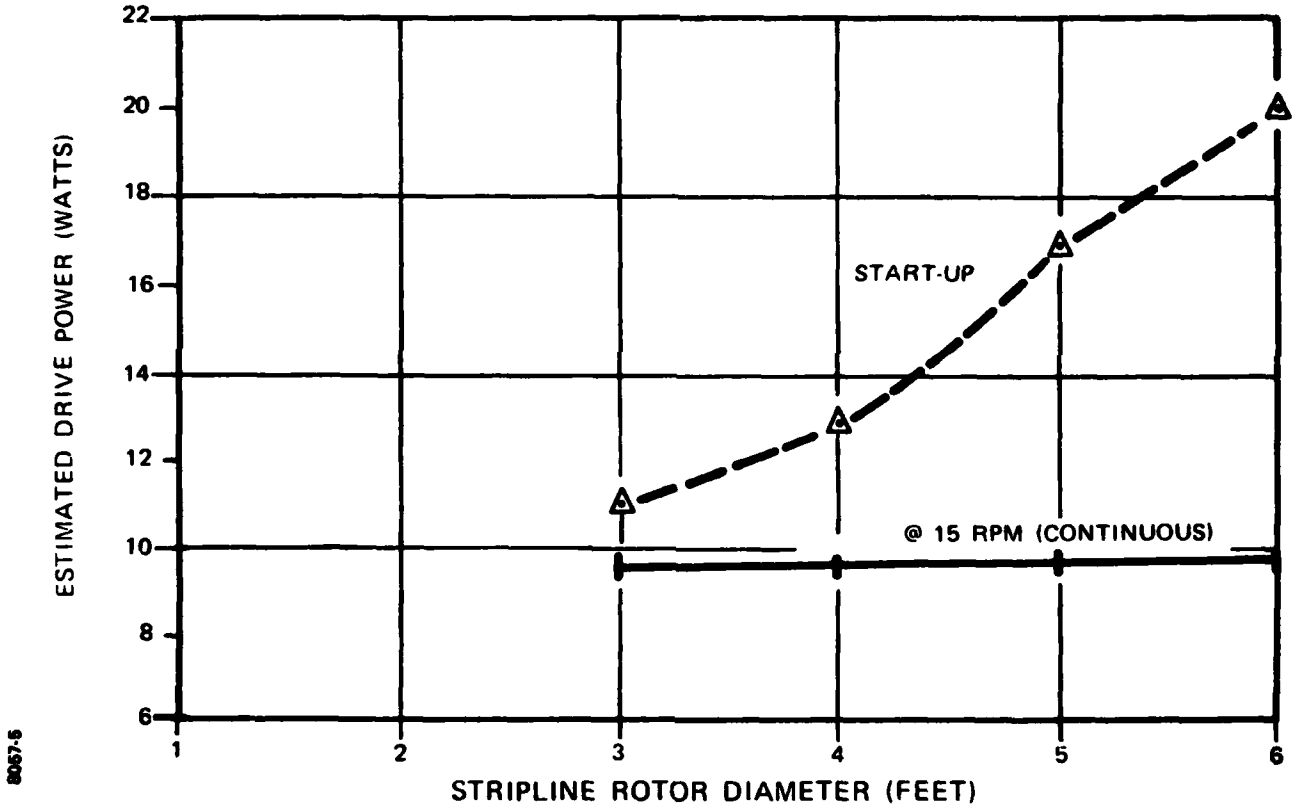

Figure 3-10. Drive Power Required as a Function of Stripline Rotor Diameter

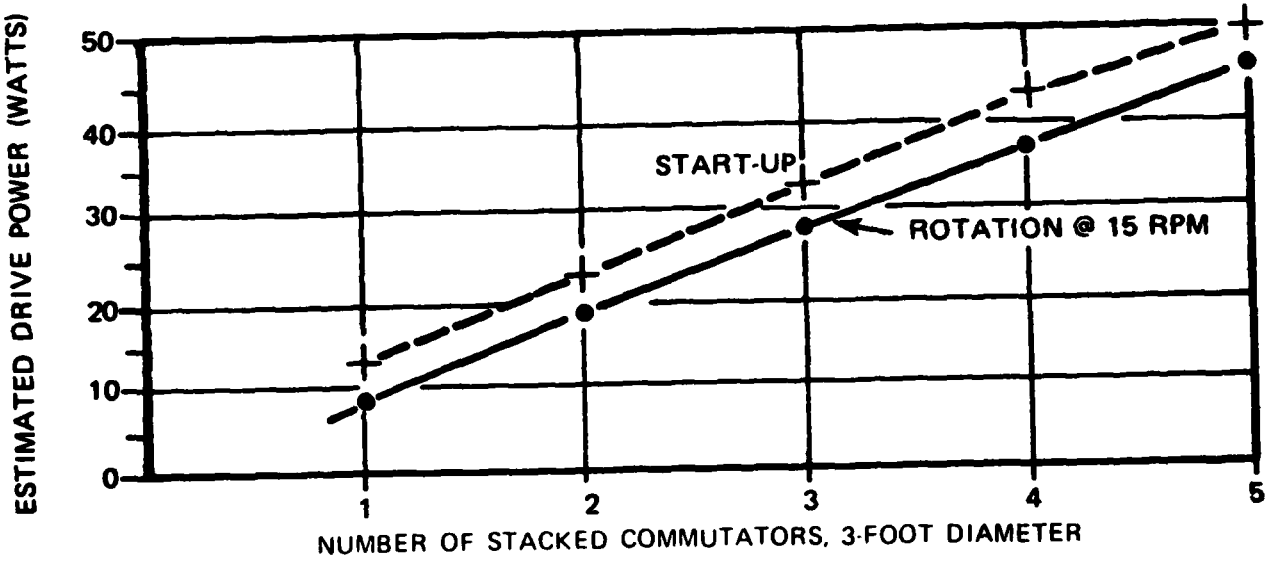

Figure 3-11. Drive Power Required as a Function of Number of Stacked 3-Foot Diameter Commutators

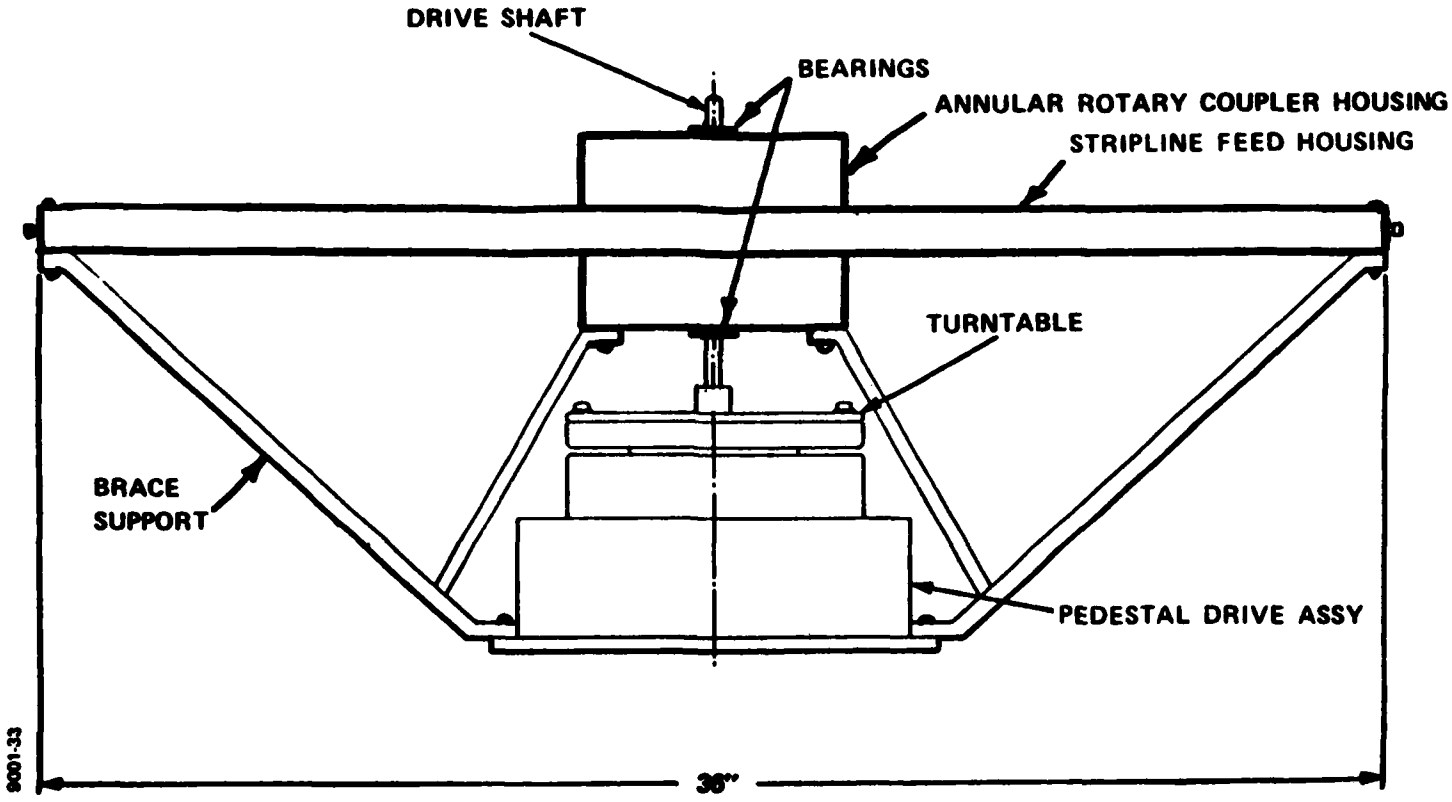

Figure 3-12. Support Structure of the Commutating Feed Assembly

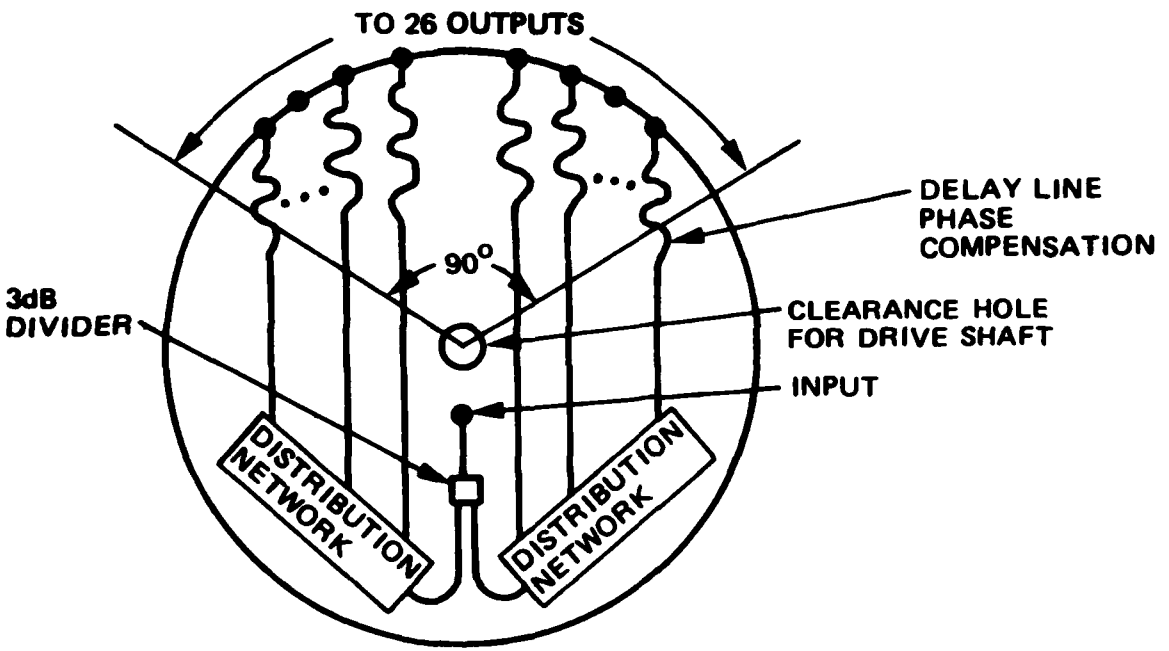

Figure 3-13. Schematic of Stripline Feed Network

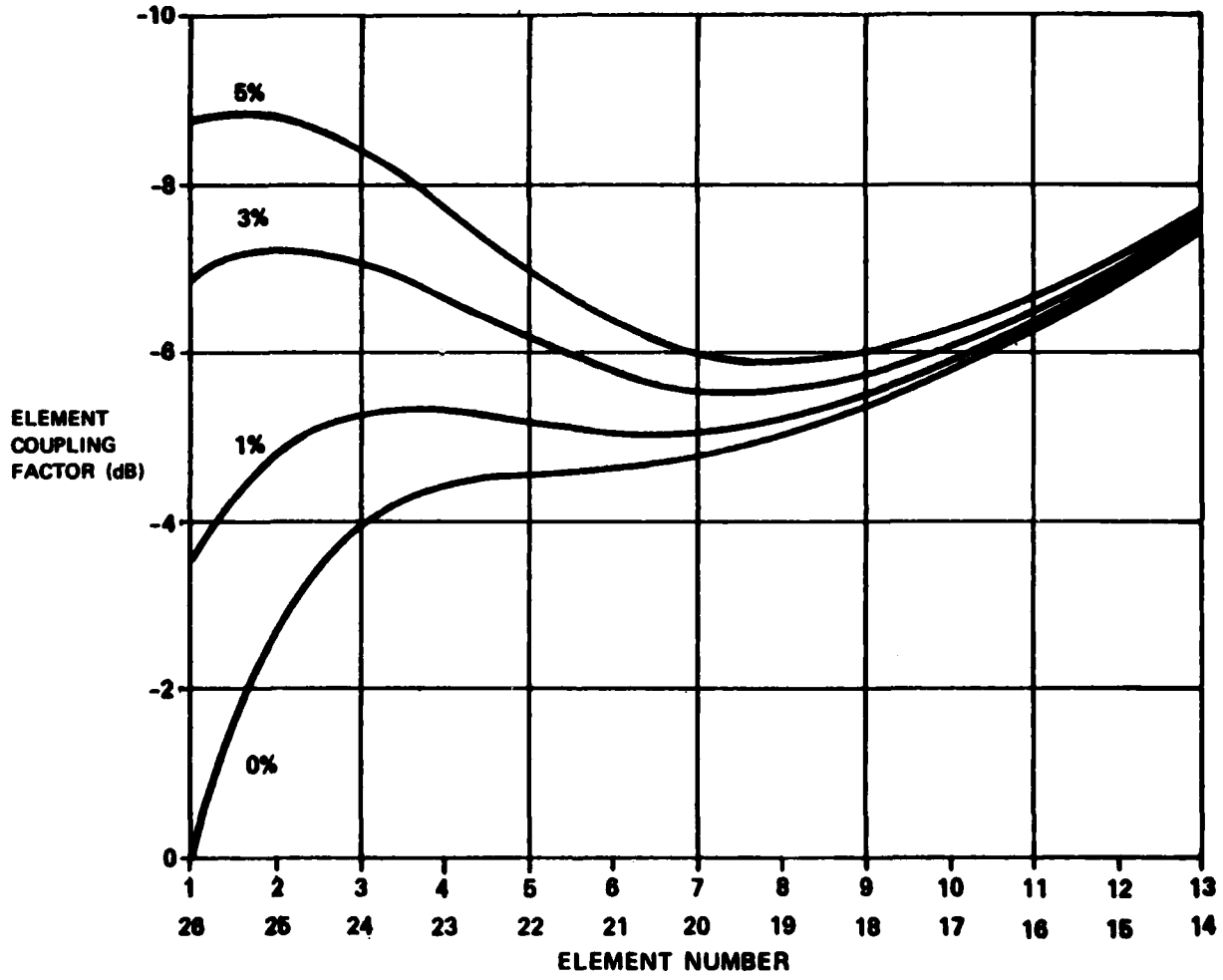

Figure 3-14. Element Coupling Factor vs. Element Number with Percent Power into End Load as Parameter

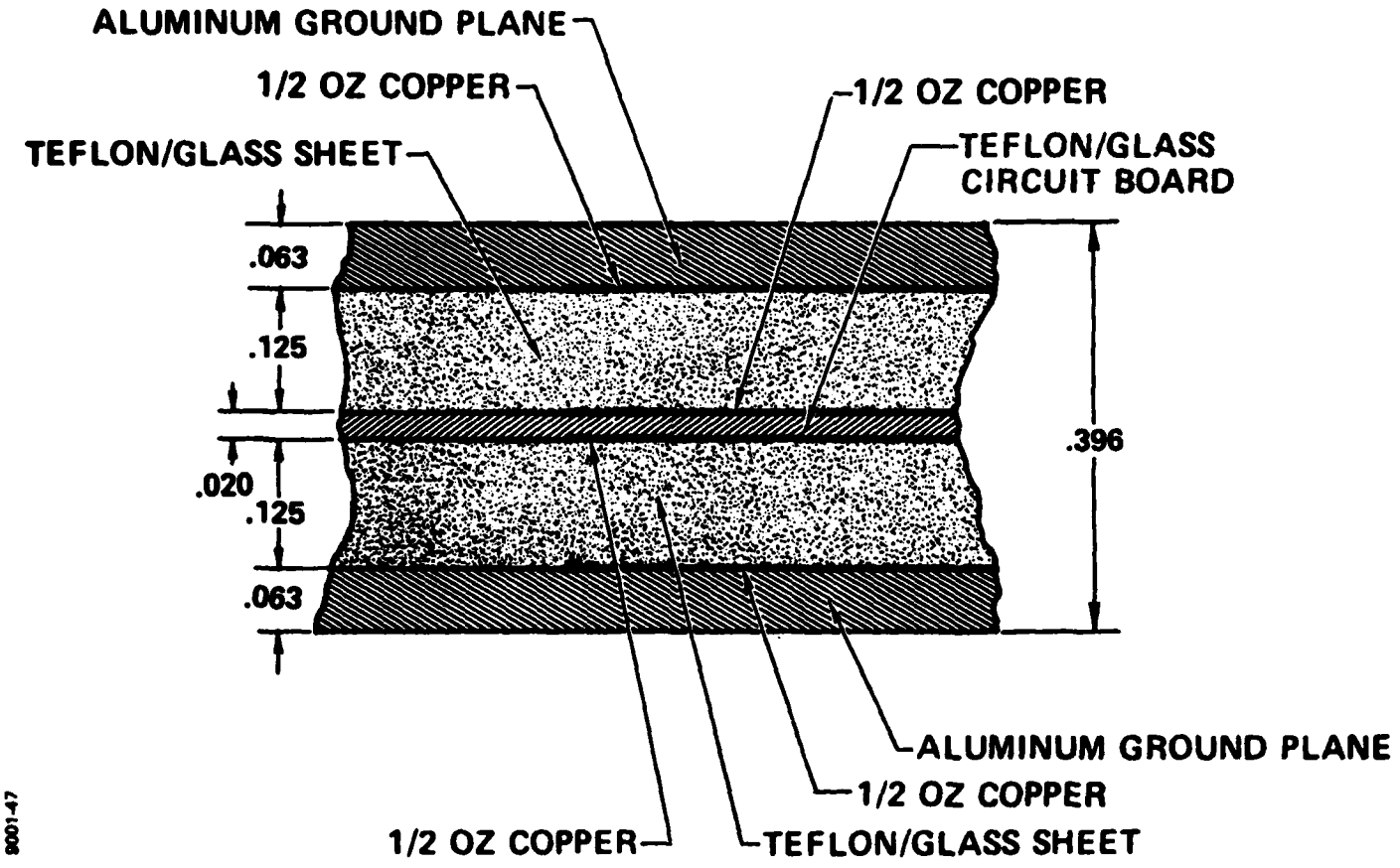

Figure 3-15. 3-Layer Stripline Configuration

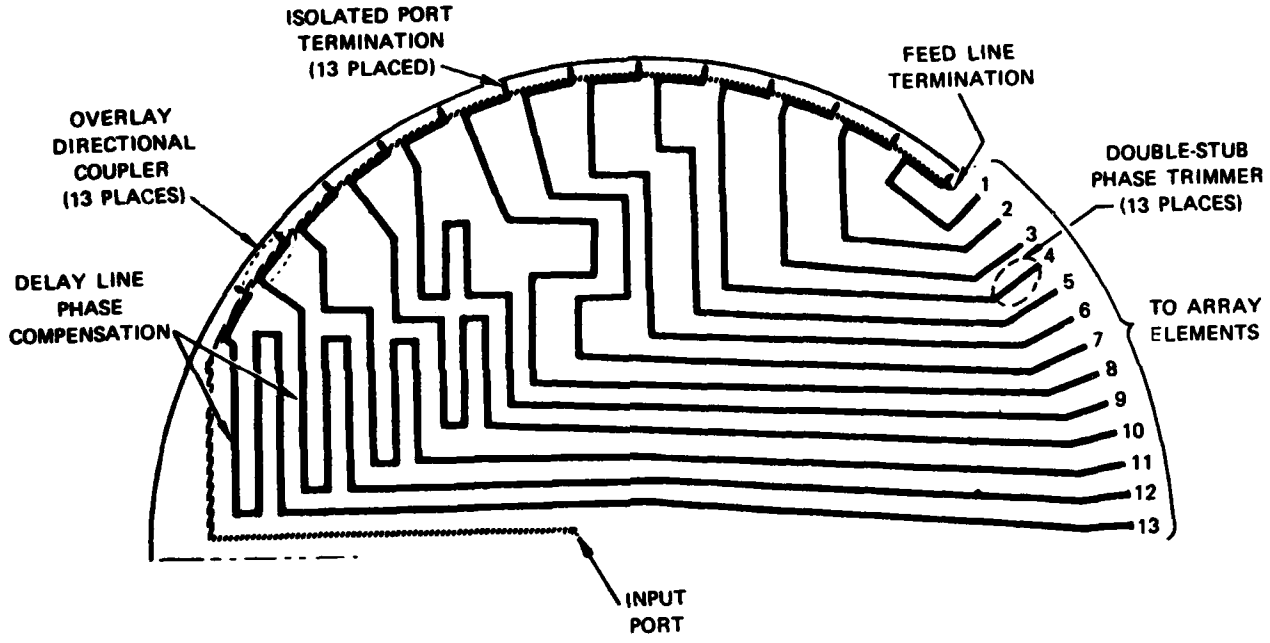

Figure 3-16. Stripline Feed Network Showing Delay Line Compensation

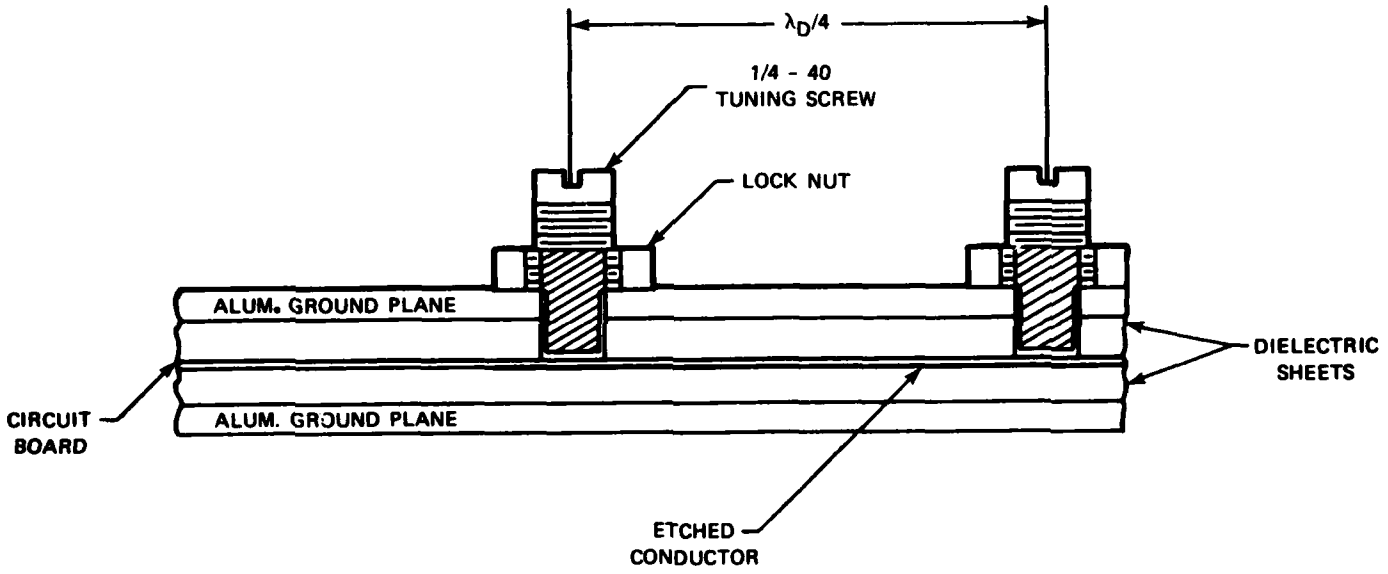

Figure 3-17. Double-Stub Phase Trimmer

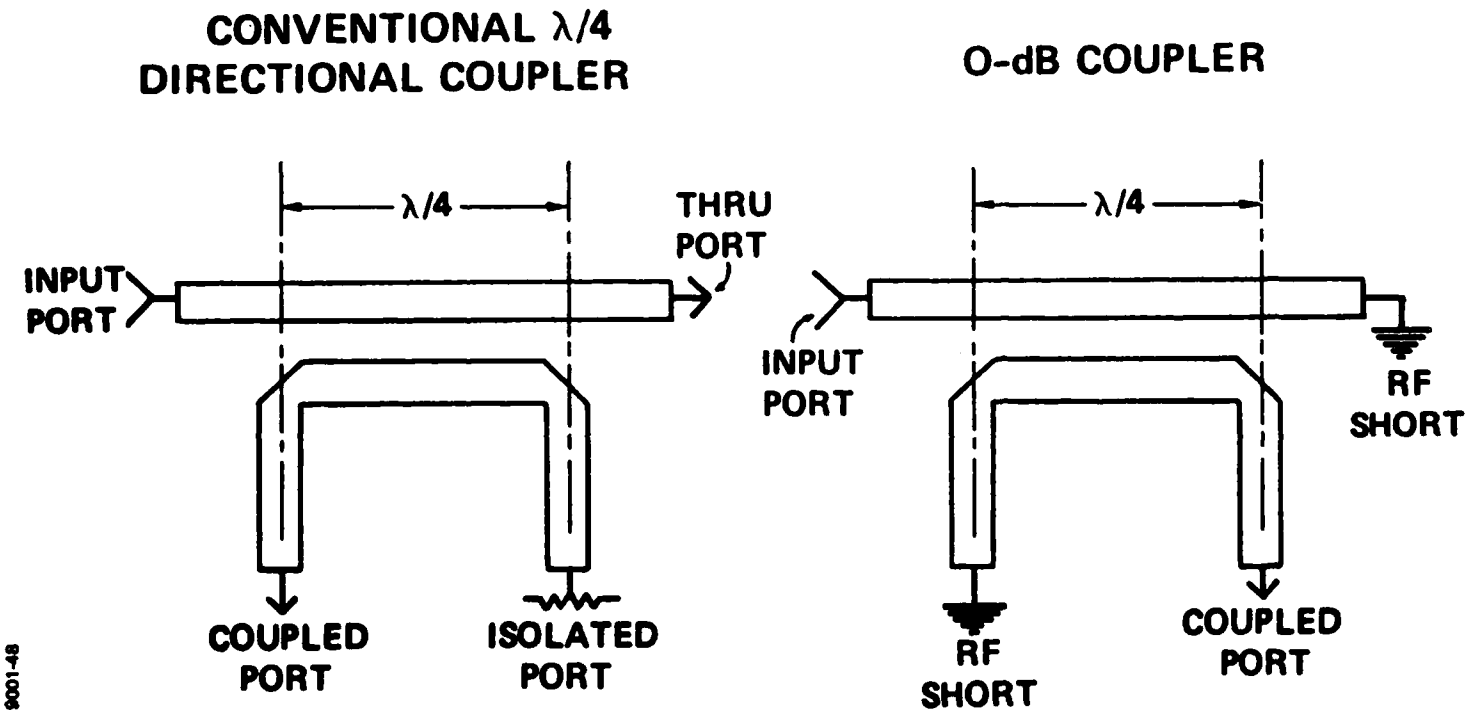

Figure 3-18. Modification of Conventional λ/4 Directional Coupler to Obtain 0-dB Coupler

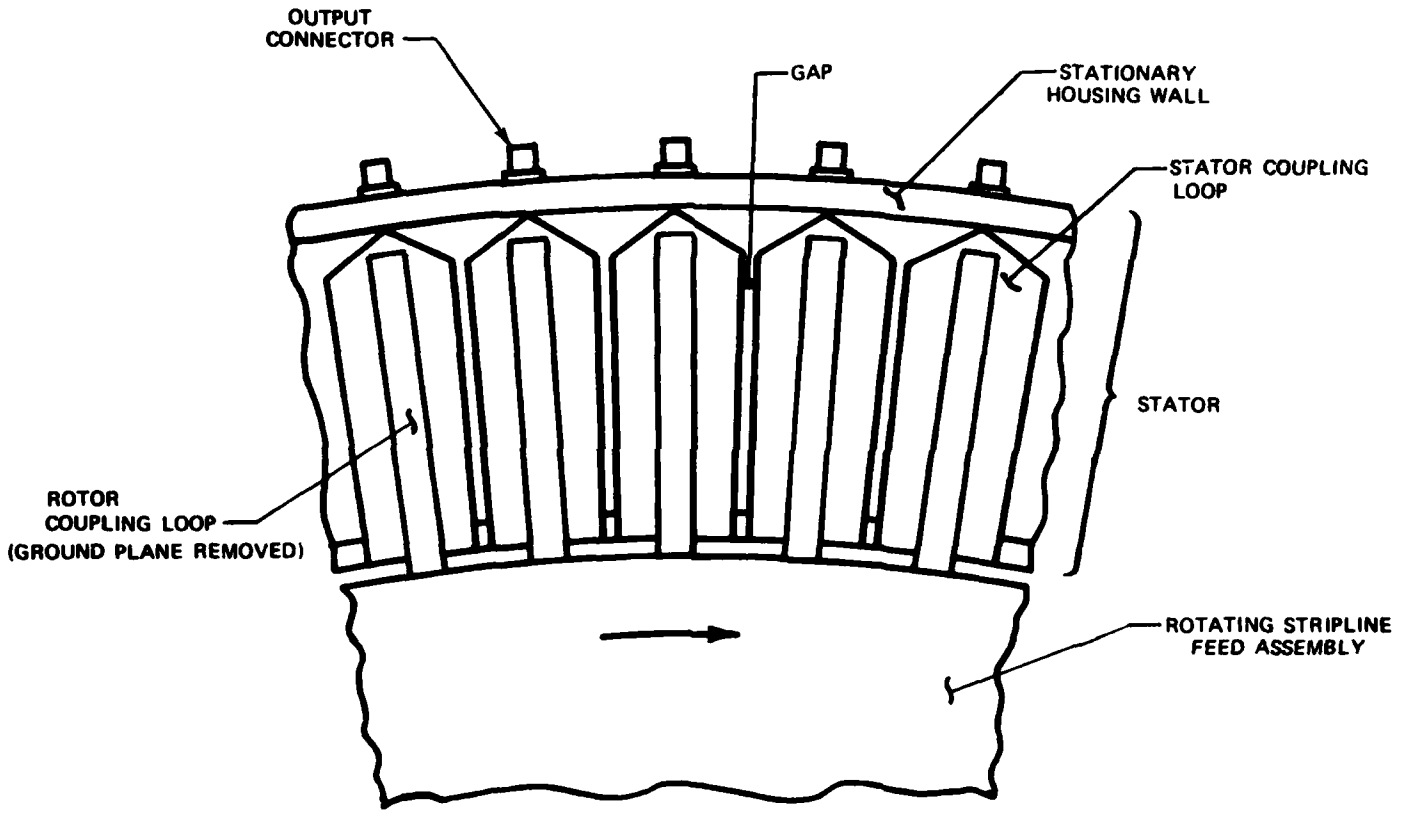

Figure 3-19. Plan View of Loop-Coupling Region

SECTION 4

GENERAL METHODOLOGY AND PROPOSED SOLUTIONS

A simplified block diagram of the commutator is shown in Figure 4-1. The annular rotary coupler is a special design that provides the power-splitting function with two equal-amplitude, in-phase outputs. The rotating stripline feed network consists of a center-fed array of directional couplers, delay lines for phase compensation, phase trimmers, and printed-circuit rotor coupling loops. The stationary housing includes the support structure, pedestal drive assembly, bearings, RF chokes, stator coupling loops, and output connectors.

A flow chart of the general methodology for development of the commutator is shown in Figure 4-2. This development requires a combination of analysis, synthesis and empirical validation of results at well defined checkpoints during the development cycle. Initially, overall system requirements are allocated at the subsystem or component level. Tradeoffs are then conducted at these levels to realize a design that is capable of meeting performance and operational requirements, while minimizing production cost and risk. These tradeoffs must be made with caution, however, as results depend to a large degree on the selection criteria that are used.

The commutator development can be divided into three major design tasks: the power train, the stripline feed network, and the loop couplers. The design methodology and proposed solutions for each of these is discussed below.

4.1 Power Train

The design of the power train is straightforward. The size estimate of the rotating section, 36 inches diameter by 0.4 inch thick, is adequate for determining bearing requirements and motor size. The rotator/pedestal drive assembly required for this rotating load is purchased from a company that specializes in the design and manufacture of torque-motor driven pedestals. The model selected is a modification of an existing rotator design; thus, little risk is involved.

4.2 Stripline Feed Network

This part of the development demands the largest effort; however, the technology required is well known and readily available. Basic design information for the overlap directional couplers is described in the literature[1]; however, a modified configuration with the load arm crossing over the through line requires additional experimental data.

In order to establish a performance baseline, the tabulated design information[1] is used to make three overlap directional couplers of the conventional configuration, with nominal coupling values of -5.0, -6.5, and -8.0 dB. This step is essential to reconcile small yet significant differences between tabulated parameters and those actually used, such as relative dielectric constant, ground-plane spacing, center-board thickness, and copper thickness. Next, a -6.5 dB coupler with the load arm "flipped" is built, and the coupling, VSWR and isolation as a function of frequency are compared to the baseline design. Dimensional changes are made to compensate for the additional capacitive loading at the load-part crossover, and matching is improved until acceptable values of coupling flatness, VSWR, and isolation are obtained. After several iterations, the design is optimized for several coupling values over the desired range: -5.0, -6.5, and -8.0dB. Thus, an accurate design curve of coupling value versus overlap is derived for the particular coupler geometry to be used. To double-check the accuracy of this design information, a test fixture consisting of a portion of the 13-element series feed is built and evaluated. The last five couplers, for elements 9 through 13, are chosen as these cover nearly the entire range of coupling values, and require the least area when the proper delay line phase compensations are included. In addition to demonstrating the performance of several couplers connected in series, this stripline test fixture also allows design verification of delay lines, phase trimmers, flange-mounted load terminations, and line losses in the stripline medium. Next a complete 13-element series feed network, including the rotor loop couplers, is built and evaluated. This provides

---

1. H. Howe, Jr., "Stripline Circuit Design," Artech House, Inc., Dedham, Ma., 1974, pp. 126, 132-150, 153-157.

---

a final opportunity for minor design changes to optimize the rotating stripline assembly before fabricating the prototype commutator. This test fixture will also be used for power-handling capability tests, which can be conducted most economically at this stage of the hardware development.

4.3 Loop Couplers

The non-contacting magnetic loop-coupler configuration proposed is basically a new concept; however, much of the technology used is available: $\lambda/4$ directional couplers, parallel-plate balun loop-couplers, and double quarter-wavelength RF chokes.

The approximate performance of the loop couplers can be surmised by modifying analytical expressions that describe broadside coupled lines [2]. To achieve highly-efficient, wideband, power transfer there exist a multitude of parameters that require optimization: the length, width and ground-plane spacing of both the rotor and stator loops, the gap between adjacent stator loops, and most critically, the separation between rotor and stator loops.

An excellent starting point for the stator loop-coupler design is a balun loop-coupler developed by ITT Gilfillan for a 110-way parallel-plate radial line combiner that operates over the 1.2 to 1.4 GHz band. The length, ground-plane spacing, and gap between adjacent loop couplers remains unchanged, while the width is reduced by 12.7% to account for differences between combiner and commutator in diameter and number of loop couplers, 110 versus 100.

Once the stator loop-coupler design is fixed, a relatively simple test fixture is built that allows the width and ground-plane spacing of the rotor loop-coupler, as well as the gap between rotor and stator, to be varied. In order to limit the number of variables to be optimized at one time, the rotor loop-coupler RF grounds are made using beryllium-copper spring contacts, rather than non-contacting RF chokes. After the optimum rotor

---

2. Cohn, S. "Characteristic Impedance of Broad Side Coupled Strip Transmission Lines," IEEE Trans. Microwave Theory Tech., vol. MTT-8, pp. 633-637, 1960.

---

loop-coupler width and ground-plane spacing are found, a second test fixture with RF chokes incorporated is built to determine precisely the optimum rotor-to-stator gap setting.

Although the preceding optimizations are carried out with the rotor loops stationary, centered over the stator loops, the entire stripline section can be slowly moved by hand so that insertion loss and phase versus rotational angle can be observed.

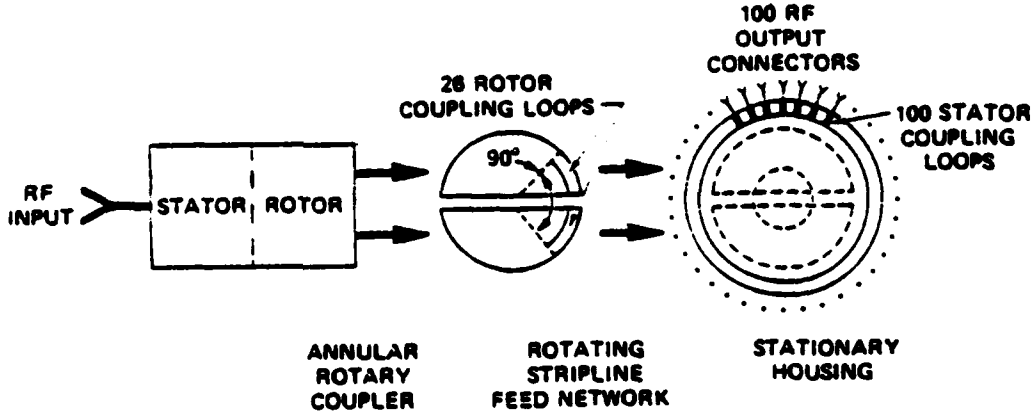

Figure 4-1. Block Diagram of Commutating Feed Assembly

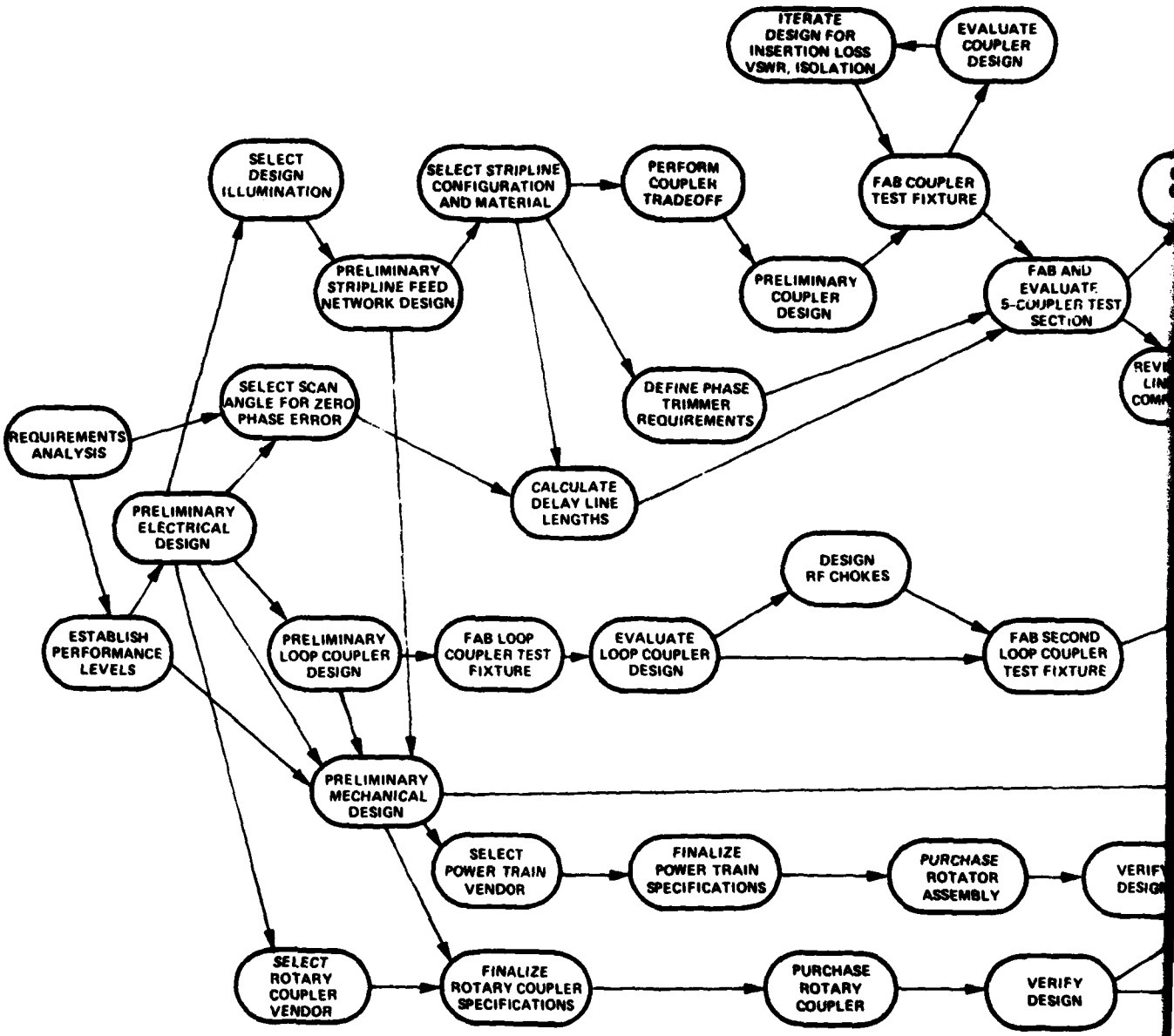
ITERATE DESIGN FOR INSERTION LOSS VSWR, ISOLATION
EVALUATE COUPLER DESIGN
SELECT DESIGN ILLUMINATION
SELECT STRIPLINE CONFIGURATION AND MATERIAL
PERFORM COUPLER TRADEOFF
FAB COUPLER TEST FIXTURE
PRELIMINARY STRIPLINE FEED NETWORK DESIGN
PRELIMINARY COUPLER DESIGN
FAB AND EVALUATE 5-COUPLER TEST SECTION
SELECT SCAN ANGLE FOR ZERO PHASE ERROR
DEFINE PHASE TRIMMER REQUIREMENTS
REQUIREMENTS ANALYSIS
CALCULATE DELAY LINE LENGTHS
PRELIMINARY ELECTRICAL DESIGN
DESIGN RF CHOKES
ESTABLISH PERFORMANCE LEVELS
PRELIMINARY LOOP COUPLER DESIGN
FAB LOOP COUPLER TEST FIXTURE
EVALUATE LOOP COUPLER DESIGN
FAB SECOND LOOP COUPLER TEST FIXTURE
PRELIMINARY MECHANICAL DESIGN
SELECT POWER TRAIN VENDOR
FINALIZE POWER TRAIN SPECIFICATIONS
PURCHASE ROTATOR ASSEMBLY
SELECT ROTARY COUPLER VENDOR
FINALIZE ROTARY COUPLER SPECIFICATIONS
PURCHASE ROTARY COUPLER
VERIFY DESIGN

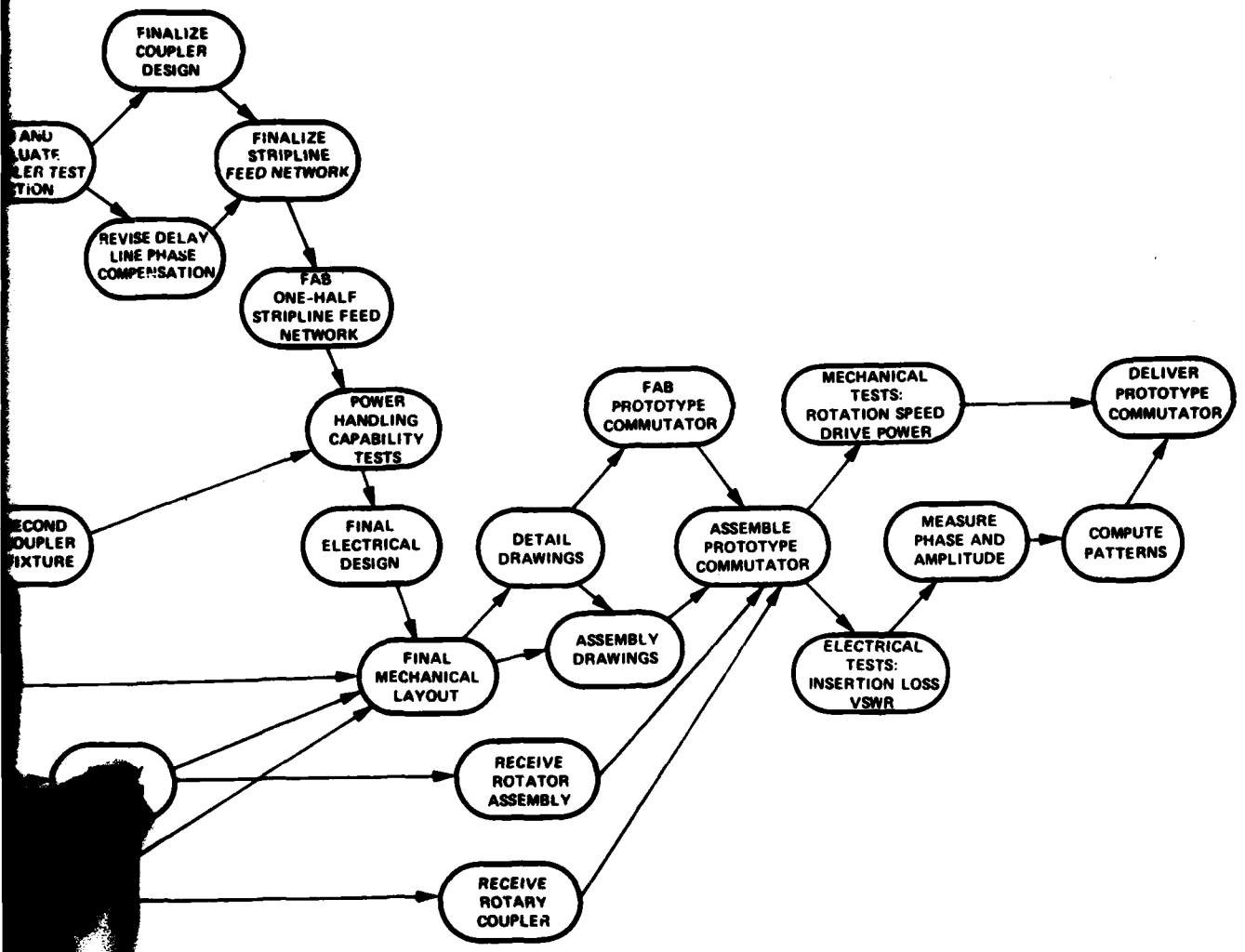

Figure 4-2. General Methodology for Development of Commutating Feed Assembly

2

SECTION 5

TECHNICAL RESULTS

5.1 Rotator Pedestal Assembly

The rotator pedestal assembly and control unit were completed and source-inspected in preparation for delivery by the vendor. During operation at 15 rpm, the turntable was observed to have a periodic flutter large enough to be troublesome. The effect, which is called "tachometer ripple", can be reduced to an acceptable level by making some modifications to the servo amplifier. A schematic diagram of the rotator controller is shown in Figure 5-1. The time constant of the RC network in the feedback loop was changed to lower the roll-off frequency of power amplifier AR1. This minor change improved performance so that there is no perceptible flutter in the pedestal turntable.

5.2 Annular Rotary Coupler

The annular rotary coupler is a modification of a unit that had originally been developed for use at the TACAN band. Changes were made to the internal corporate feeds for 1.2 to 1.4 GHz operation, and to provide two equal-amplitude, in-phase outputs. A photograph of the unit is shown in Figure 5-2.

Measured swept-frequency insertion loss and input VSWR of the rotary coupler are shown in Figures 5-3 and 5-4. The power split between outputs is excellent: within 0.05 dB over the entire range of 1.0 to 1.5 GHz. Phase difference between output ports A and B, shown in Figure 5-5, is negligible. Note that the coupler appears to be optimized at 1.2 GHz, rather than at the operating band center, 1.3 GHz. This results in higher than desirable insertion loss and VSWR at the upper band edge. It is the vendor's opinion that no substantial improvement to this particular unit could be obtained without redesign and matching of the internal parts. Expected performance of a production version of this annular rotary coupler over the 1.2 to 1.4 GHz band is 0.15 dB excess insertion loss and 1.2:1 VSWR, with usable performance at the IFF band: 0.5 dB excess insertion loss and 2:1 VSWR.

5.3 Stripline Feed Network

5.3.1 Modified Overlap Directional Coupler

The design of the modified (isolated-port arm "flipped") overlap directional coupler was optimized for three coupling values over the desired range: -5.0, -6.5, and -8.0 dB. Measured data were used to generate the design curves shown in Figures 5-6 and 5-7. The measured coupling, isolation, and VSWR for the nominal -6.5 dB coupler design are shown in Figures 5-8 and 5-9. Although this coupler was intended for the 1.2 to 1.4 GHz band only, note the excellent performance of the device over the extended band, 1.0 to 1.6 GHz.

5.3.2 Five-Coupler Stripline Test Fixture

A test fixture consisting of the last five couplers of the stripline feed network, for elements 1 through 5, was built and tested. Figure 5-10 is a photograph of this circuit. The measured insertion loss referenced to the input port, as a function of frequency is shown in Figure 5-11. The numbers in parentheses represent predicted losses which are based on the coupler design values and theoretical line losses of 0.015 dB per inch. These results are summarized in Table 5-1.

Table 5-1. SUMMARY OF FIVE-COUPLER STRIPLINE TEST FIXTURE PERFORMANCE

Element	Measured Ins. Loss (dB)	Theoretical Ins. Loss (dB)	Variance (dB)
5	6.00	6.47	-0.47
4	8.00	8.27	-0.28
3	9.80	9.68	+0.12
2	10.85	10.66	+0.19
1	11.32	11.14	+0.18

On the final stripline circuit layout, a slight correction will be made to the overlap region of each coupler to keep the variance within $\pm$ 0.2 dB.

The measured swept-frequency VSWR of this test circuit is shown in Figure 5-12. The input match is less than 1.12:1 over the 1.2 to 1.4 GHz band.

5.3.3 Stripline Feed Network

A layout of the complete stripline feed network is shown in Figure 5-13. A stripline matching stub is required at the discontinuity where each rotor loop extends beyond the stripline ground planes. Note that the two halves are separate circuits that are identical mirror images of one another. The two stripline assemblies, each consisting of a central 0.020-inch thick etched circuit board and two 0.125-inch thick dielectric sheets, are bonded under heat and pressure to form rugged, trouble-free units. These "unitized" stripline assemblies are then mechanically mounted between a pair of 0.063-inch thick aluminum ground planes, approximately three feet in diameter, to form the rotating feed network which is shown mounted in the stationary housing, Figure 5-14.

Artwork for the stripline feed network has been completed, and fabrication of these parts is scheduled for late August.

5.3.4 Delay Lines

The double-stub phase trimmers, shown earlier in Figure 3-17, were incorporated and evaluated in the five-coupler stripline test fixture. Phase adjustment of greater than 15° was measured at the midband frequency, 1.3 GHz.

5.3.5 Flanged 50-Ohm Loads

The 50-ohm load termination selected for this application is shown in Figure 5-15. The device is rugged and compact, and can be externally mounted to the stripline assembly, where it is readily accessible. With 3% power into the main-line loads, or 7.5 watts average each, the 25-watt rating of the load provides adequate margin for this design. Swept-frequency VSWR of the load, measured in a stripline test

circuit, is shown in Figure 5-16. Table 5-2 summarizes the characteristics of the load.

Table 5-2. SUMMARY OF FLANGED 50-OHM LOAD CHARACTERISTICS

Frequency of Operation	DC to 4.0 GHz
Resistor Value	50 $\pm$ 2.5
VSWR	1.3:1 Maximum
Power Dissipation	25 watts *

* De-rate to zero watts at 150°C case temperature.

5.4 Loop Couplers

5.4.1 *Loop-Coupler Test Fixture*

The design of the rotor and stator loops was optimized with the use of several test fixtures, the first of which is shown in Figure 5-17. Five rotor loops of different widths from 0.2 to 0.4 inch can be seen. This test fixture is constructed such that the ground-plane spacing of the rotor loops, as well as the separation between rotor and stator loops, can be varied. For simplicity, the RF shorts between the rotating and fixed sections were made using adjustable spring contacts rather than non-contacting RF chokes. The measured swept-frequency insertion loss for the 0.25-inch wide rotor loop, positioned directly over a stator loop, is shown in Figure 5-18. The two deep resonances at 1.05 and 1.60 GHz are due to the RF shorting arrangement used in this test fixture. Note that insertion loss of less than 0.2 dB can be achieved over a 200 MHz band.

5.4.2 RF Chokes

A second loop-coupler test fixture that includes upper and lower RF chokes was built. A cross section of this test fixture, seen in Figure 5-19, shows how the folded choke sections are implemented. The upper RF choke, with cover removed, is shown in Figure 5-20. The dark areas at the ends of the cavity are RF absorber, used to eliminate reflections that might arise from a circumferential mode. Figure 5-21 shows the upper

RF choke with the cover plate assembled, and Figure 5-22 shows a close-up view of the baseplate with stator loops and lower RF choke.

The measured swept-frequency insertion loss of the second loop-coupler test fixture is shown in Figure 5-23. Note that the deep resonances that existed with the first test fixture are gone, and the insertion loss is only 0.3 dB from about 1.15 to 1.45 GHz.

The coupling performance varies somewhat as the rotor loops pass over the stator loops. These variations are minimized in magnitude and duration by using narrow rotor loops and much wider stator loops. Of course, during the interval when the rotor loop is over the gap region between adjacent stator loops, it couples equally to these two stator loops; hence, the coupling falls below -3 dB. This effect is seen in Figure 5-24, which was measured at 1.3 GHz for the 0.25-inch wide rotor loop. The impact of this large amplitude change on the array pattern can be avoided either by staggering the relative location of rotor and stator loops so that all nulls do not occur simultaneously, or by transmitting and receiving only when loops are well engaged.

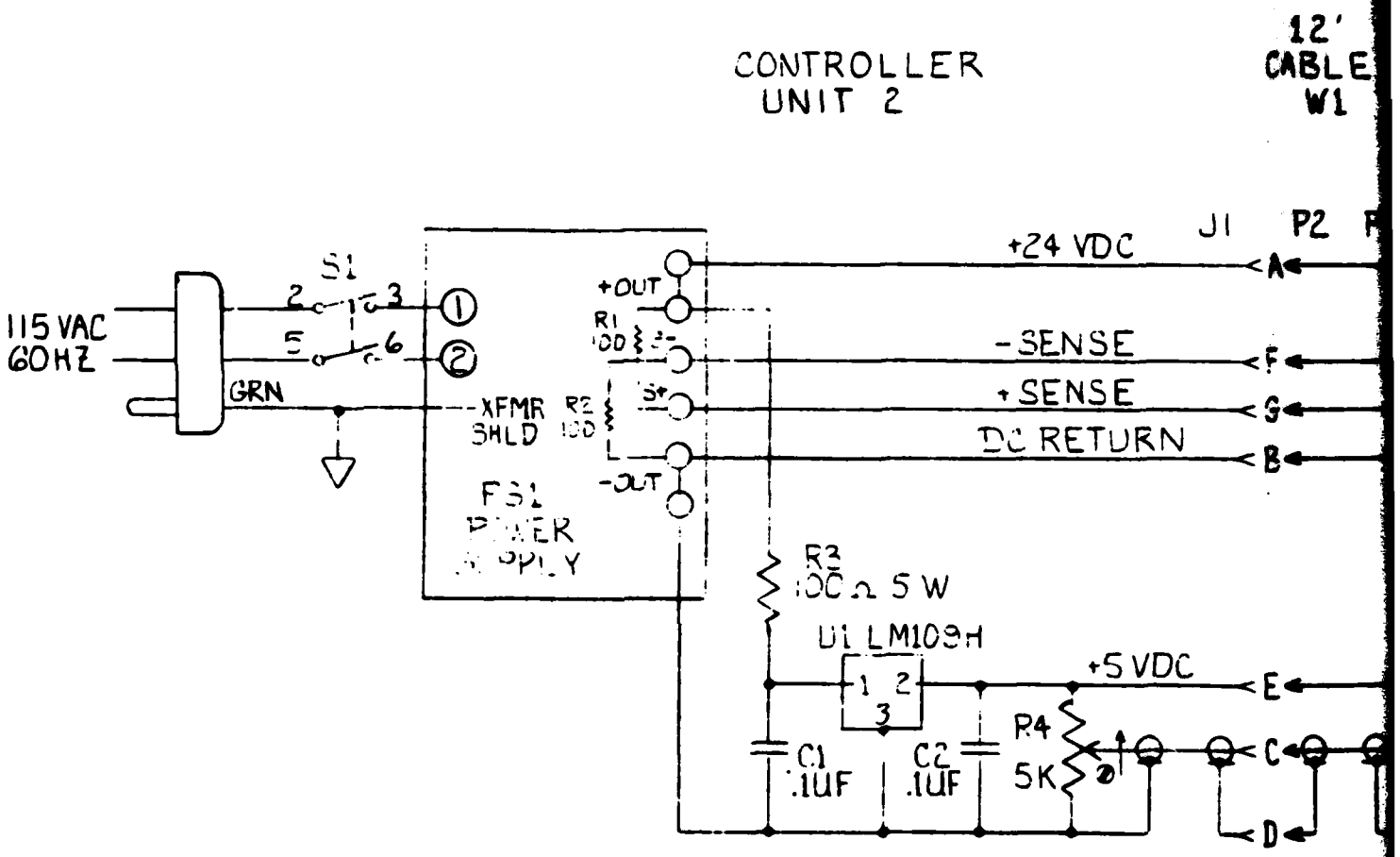
CONTROLLER
UNIT 2
12'
CABLE
W1
J1
P2
115 VAC
60HZ
S1
GRN
XFMR
SHLD
+OUT
R1
100
R2
100
-OUT
FS1
POWER
SUPPLY
+24 VDC
-SENSE
+SENSE
DC RETURN
A
F
G
B
R3
100Ω 5 W
U1 LM109H
1 2
3
+5 VDC
E
C1
.1UF
C2
.1UF
R4
5K
C
D
CLOCK, 3.6°
ZERO INDEX

E ROTATOR
UNIT 1

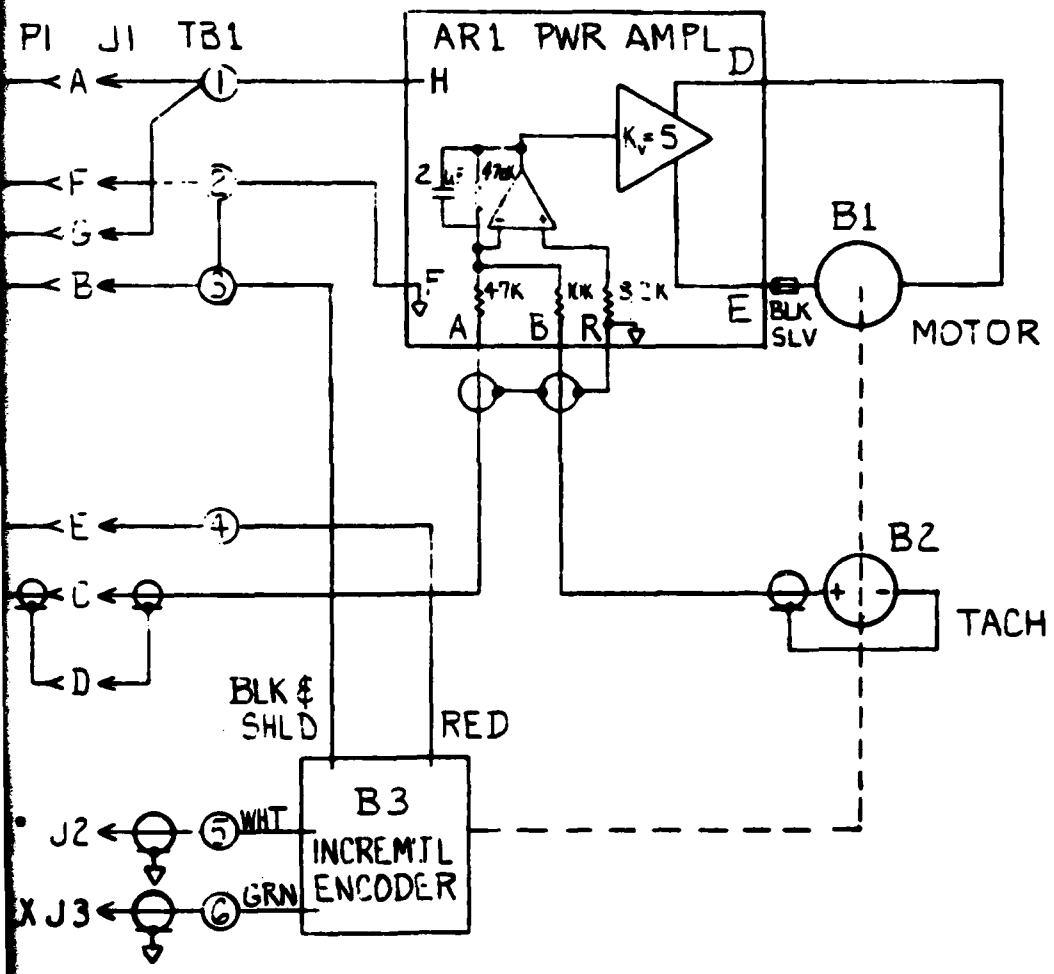

Figure 5-1. Schematic Diagram of Rotator Controller

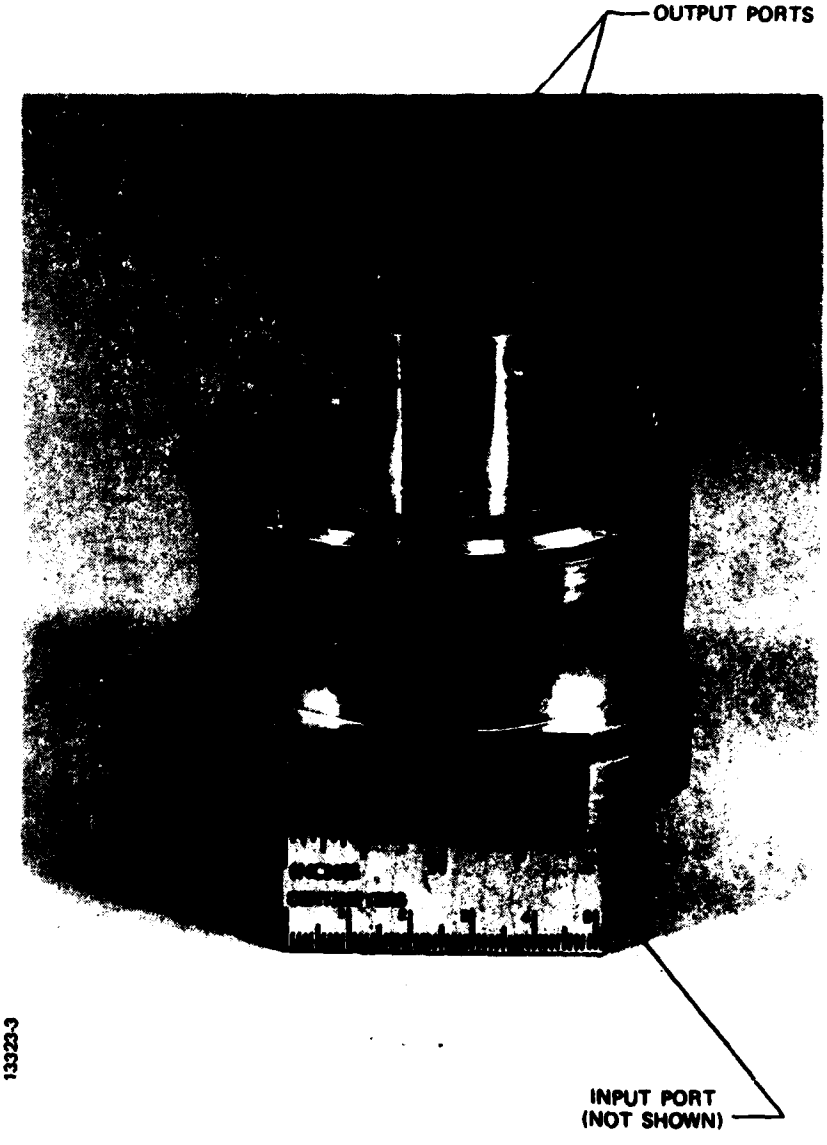

Figure 5-2. Photograph of Annular Rotary Coupler

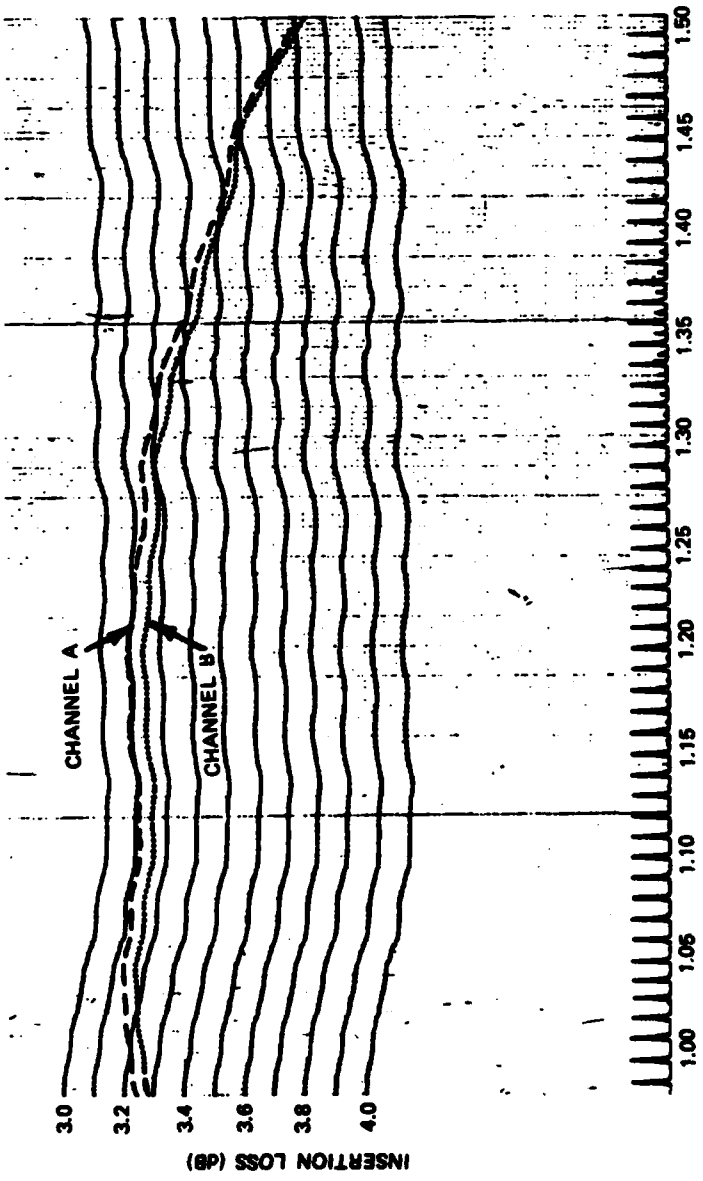

Figure 5-3. Insertion Loss vs Frequency of Annular Rotary Coupler

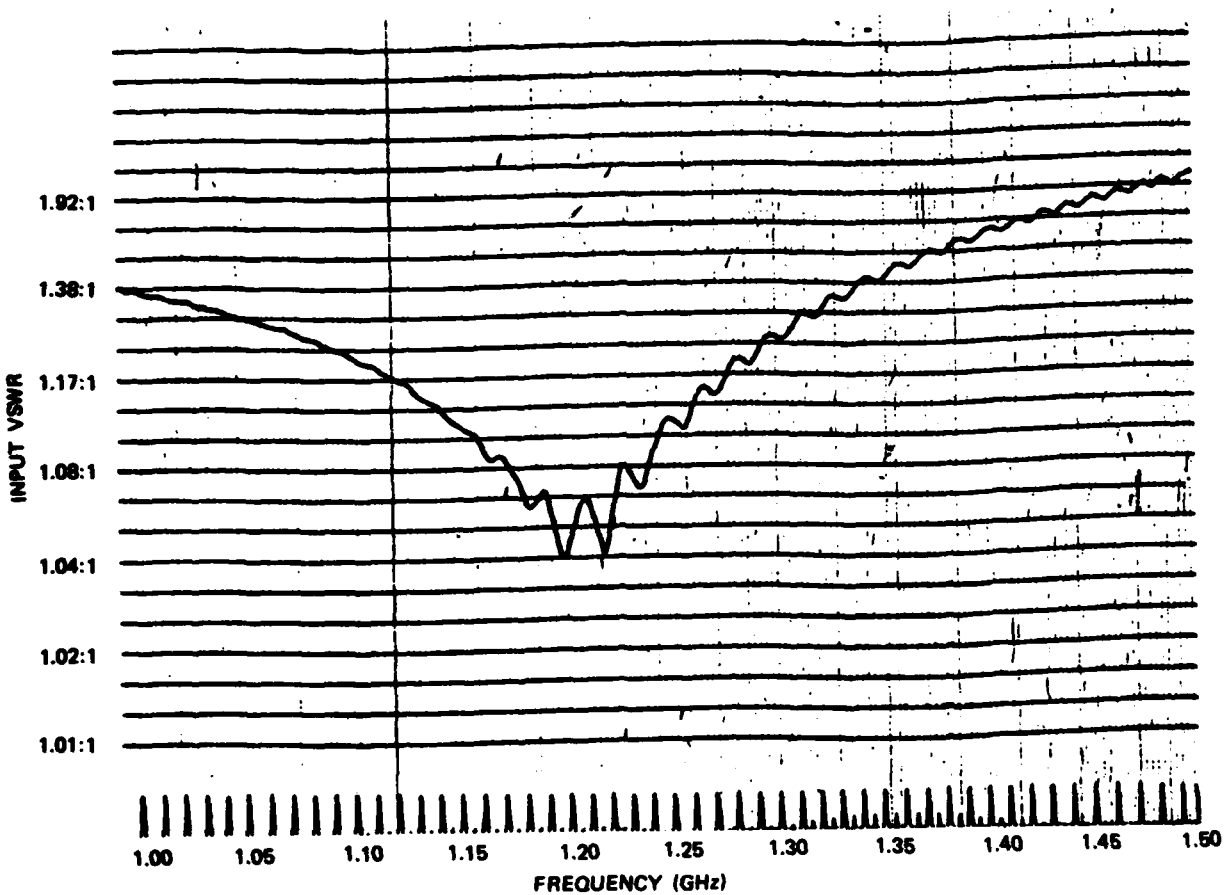

Figure 5-4. VSWR vs Frequency of Annular Rotary Coupler

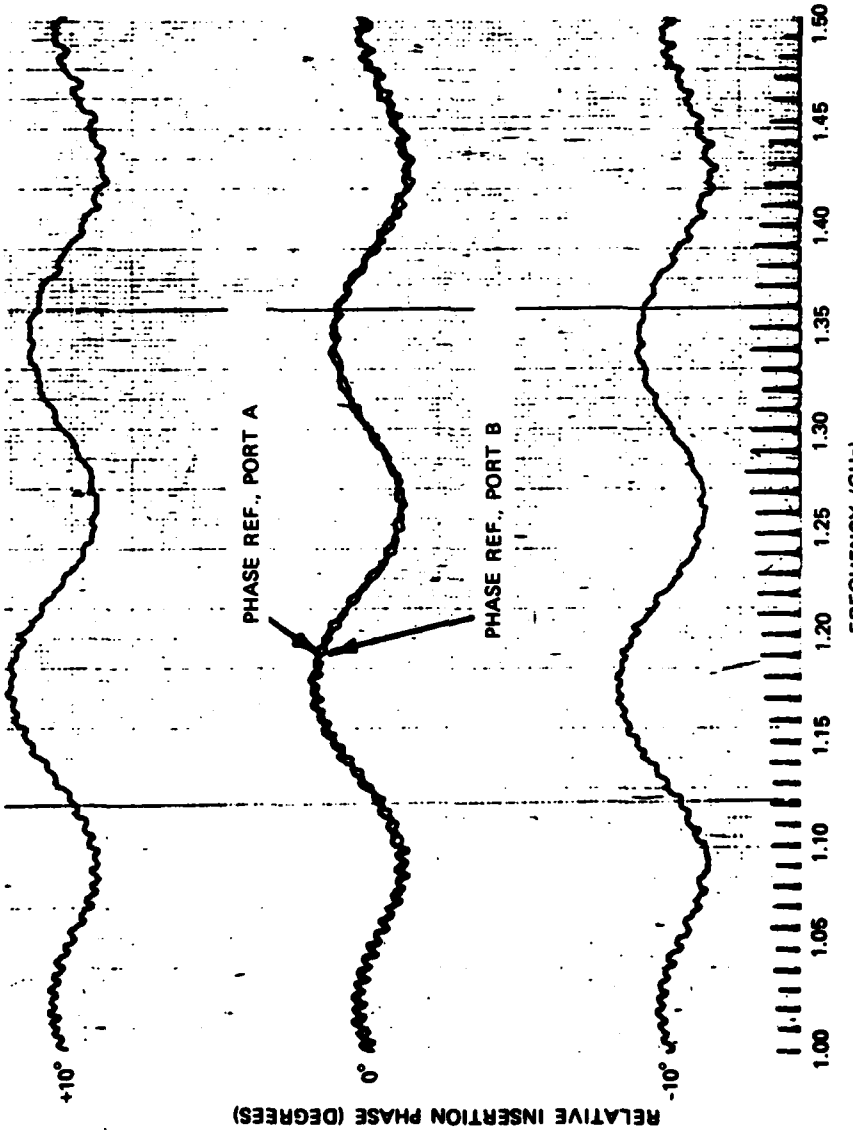

Figure 5-5. Phase Difference Between Output Ports A and B

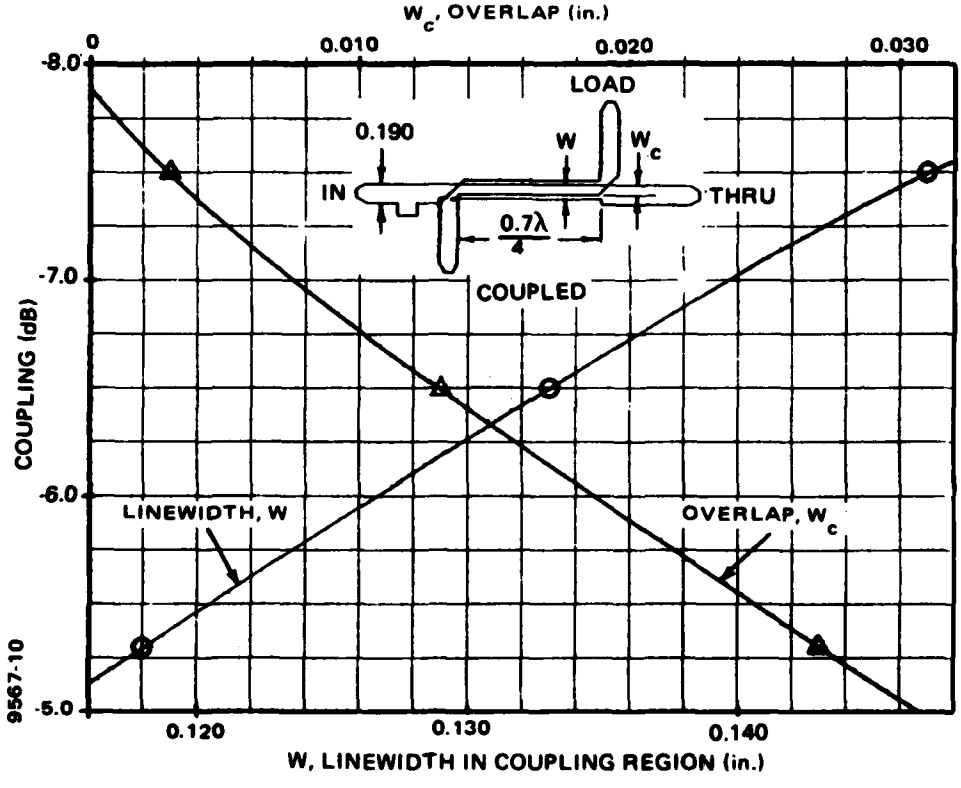

Figure 5-6. Design Curve for Modified λ/4 Overlap Directional Coupler

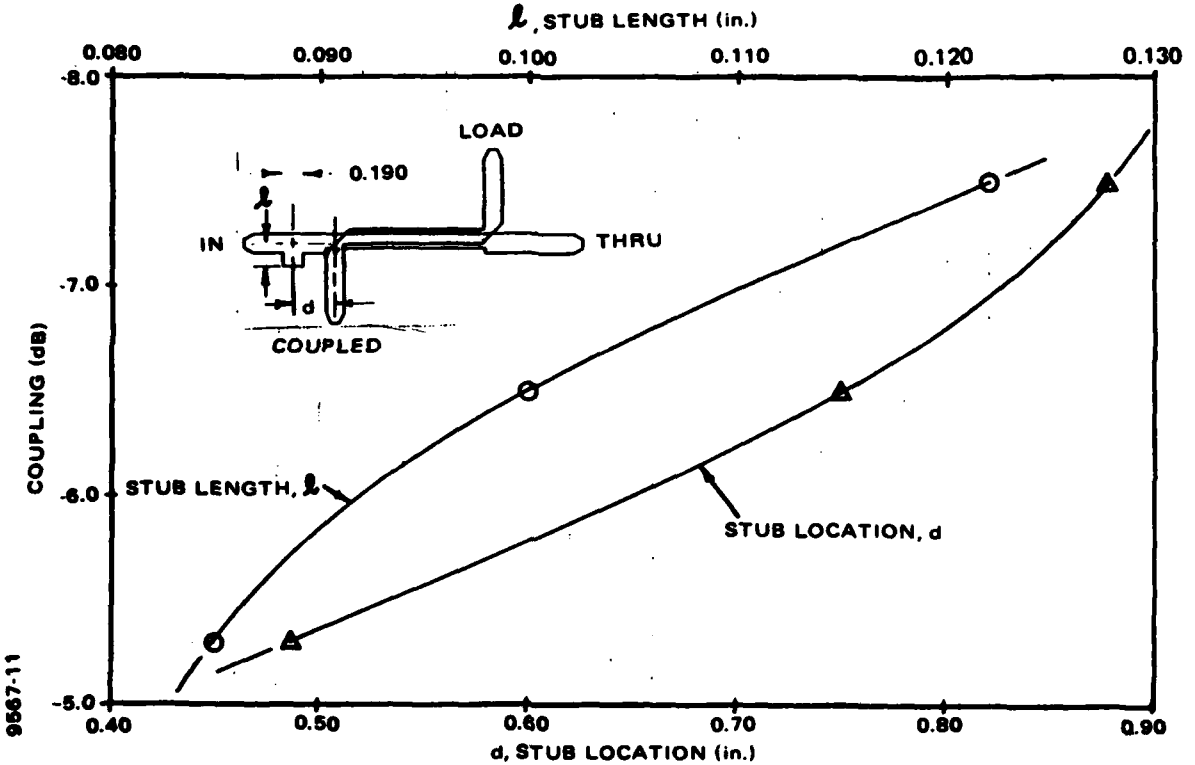

Figure 5-7. Matching Stub Length and Location

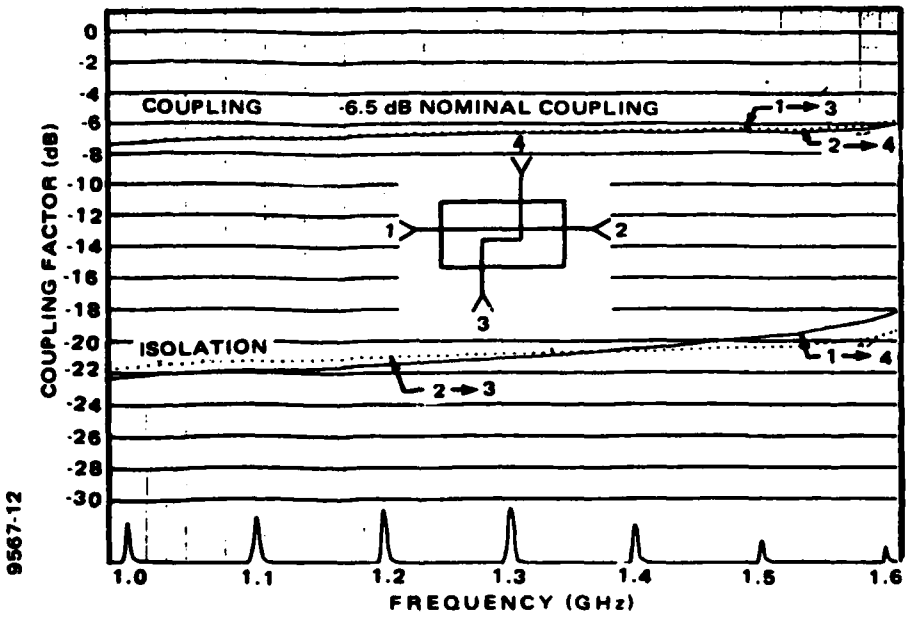

Figure 5-8. Measured Coupling and Isolation vs Frequency of Modified λ/4 Overlap Directional Coupler

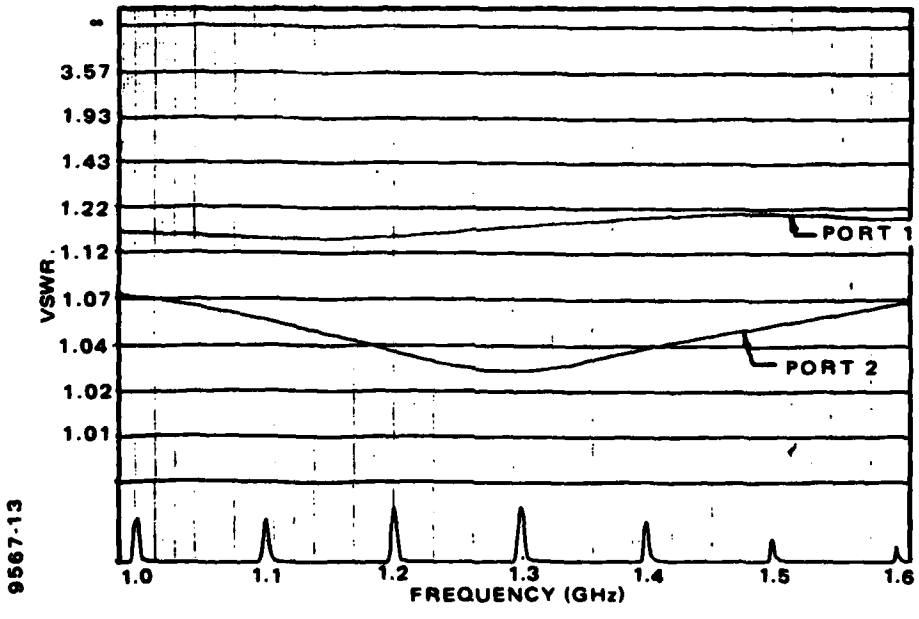

Figure 5-9. Measured VSWR vs Frequency of Modified λ/4 Overlap Directional Coupler

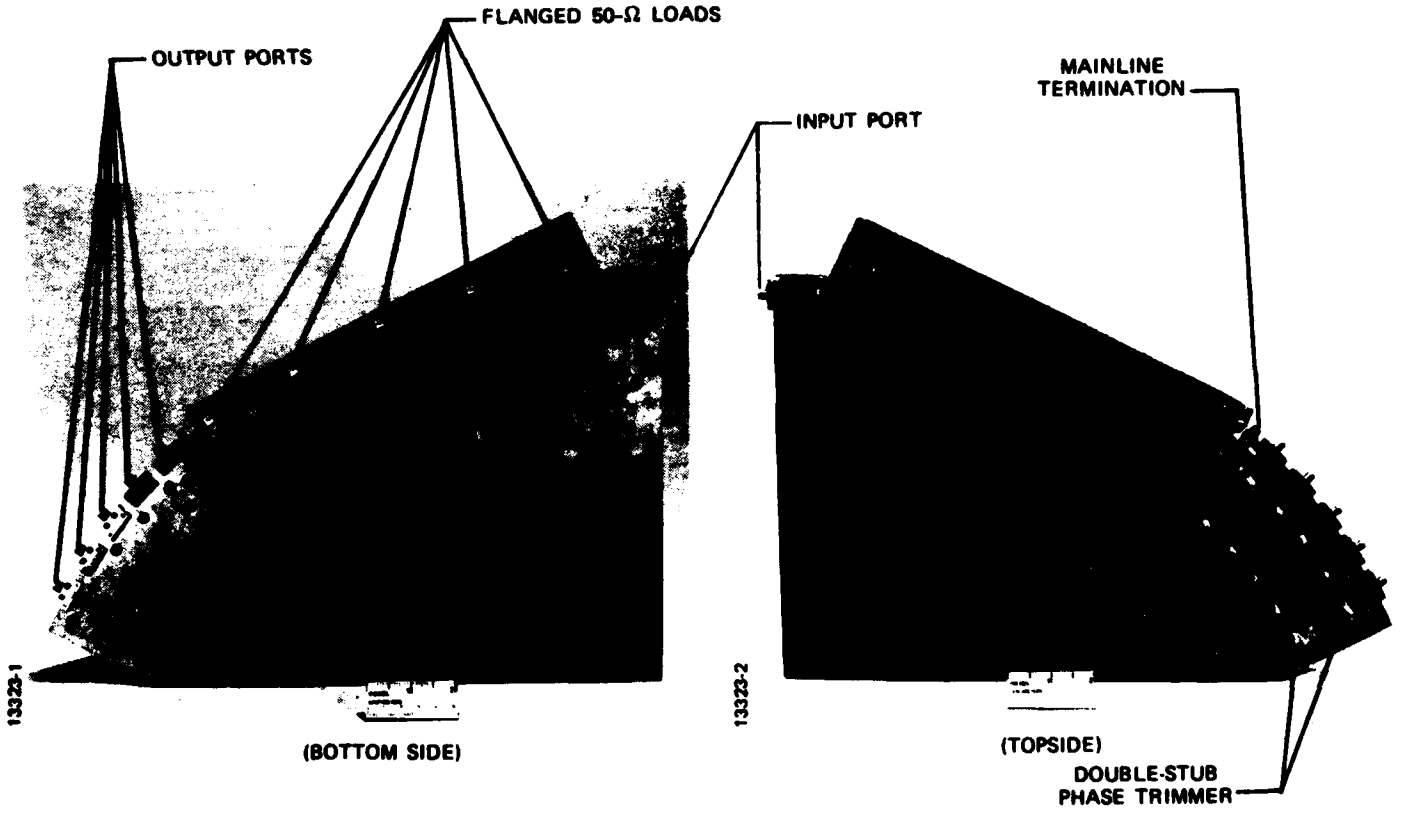

Figure 5-10. Photograph of Five-Coupler Stripline Test Fixture

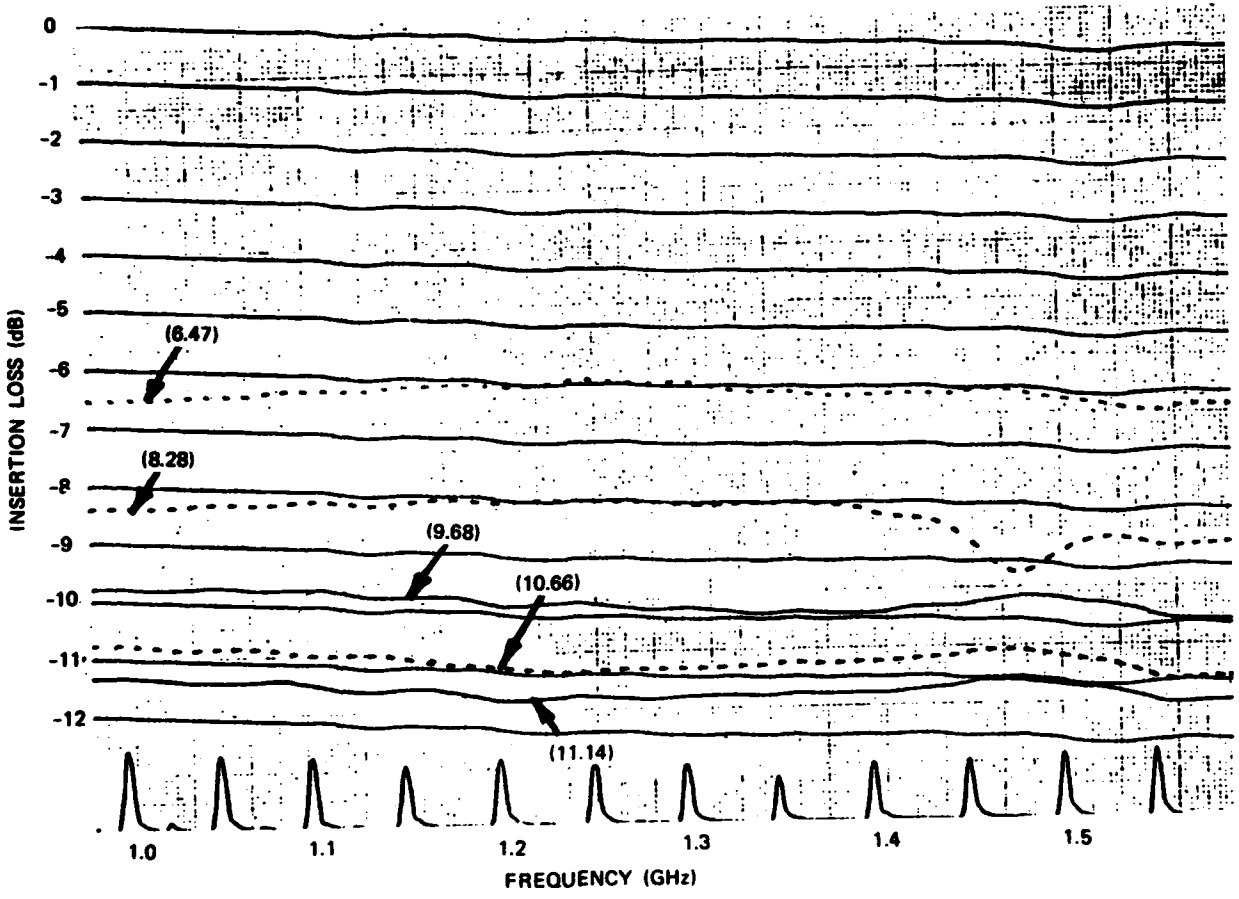

Figure 5-11. Measured Insertion Loss vs Frequency of Five-Coupler Stripline Test Fixture

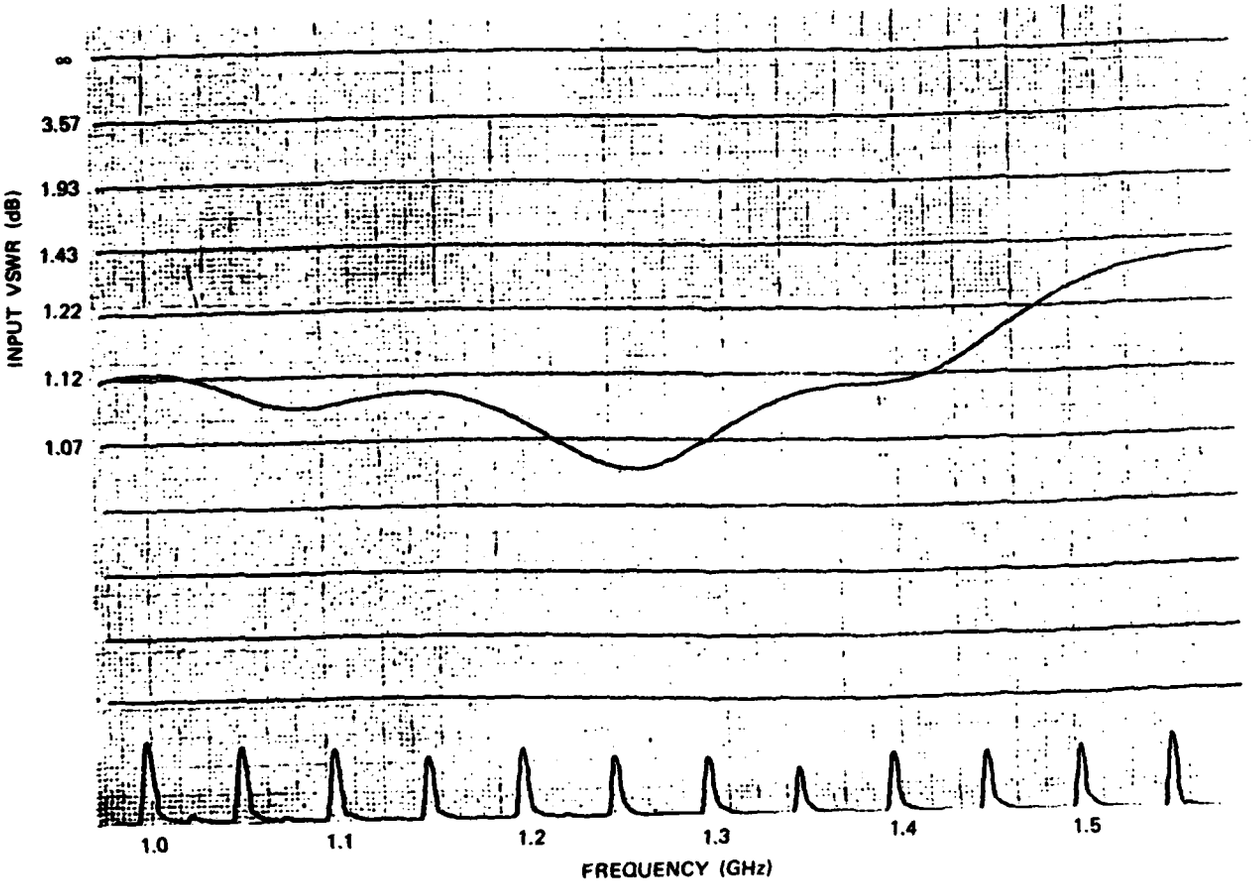

Figure 5-12. Measured Swept-Frequency VSWR of Five-Coupler Stripline Test Fixture

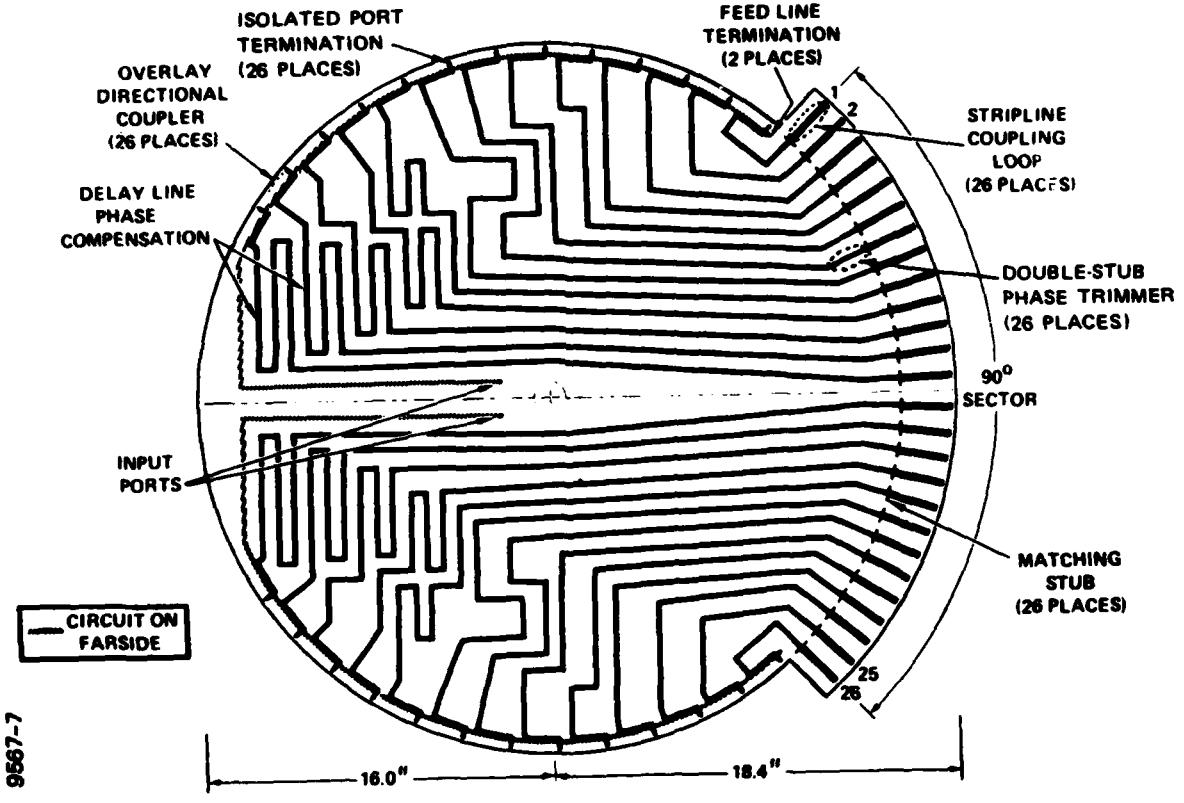

Figure 5-13. Stripline Feed Network

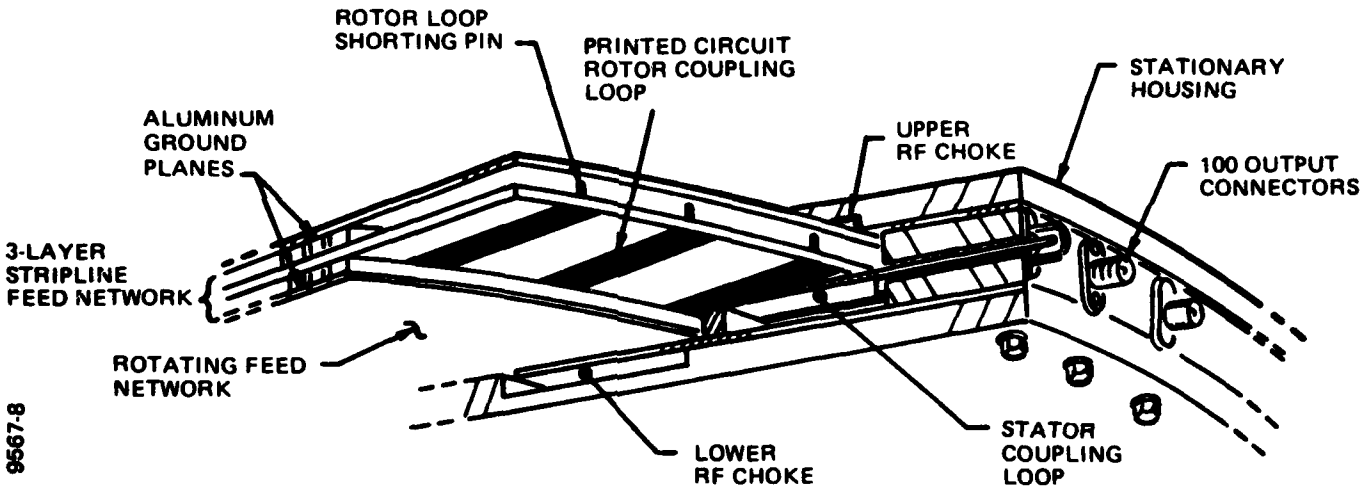

Figure 5-14. Rotating Feed Network Mounted in Stationary Housing

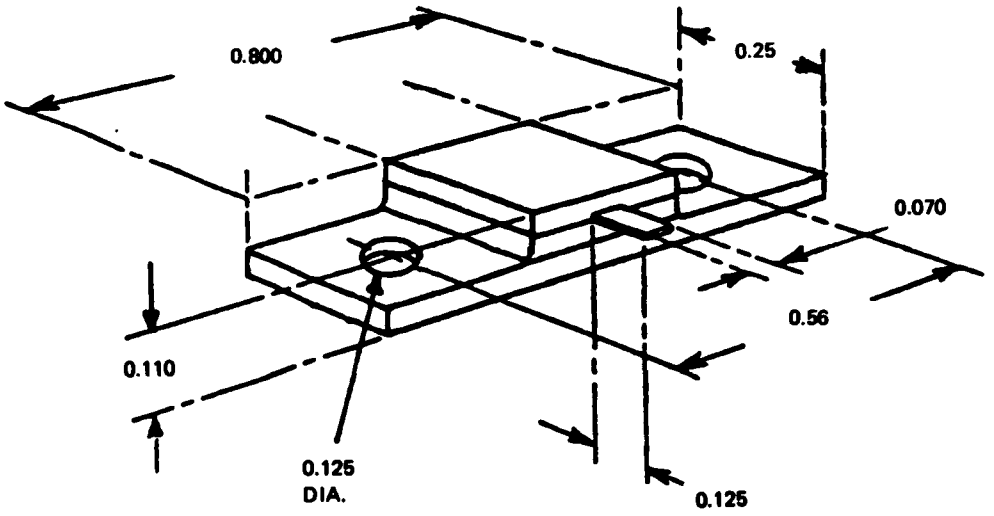

Figure 5-15. Flanged 50-Ohm Load

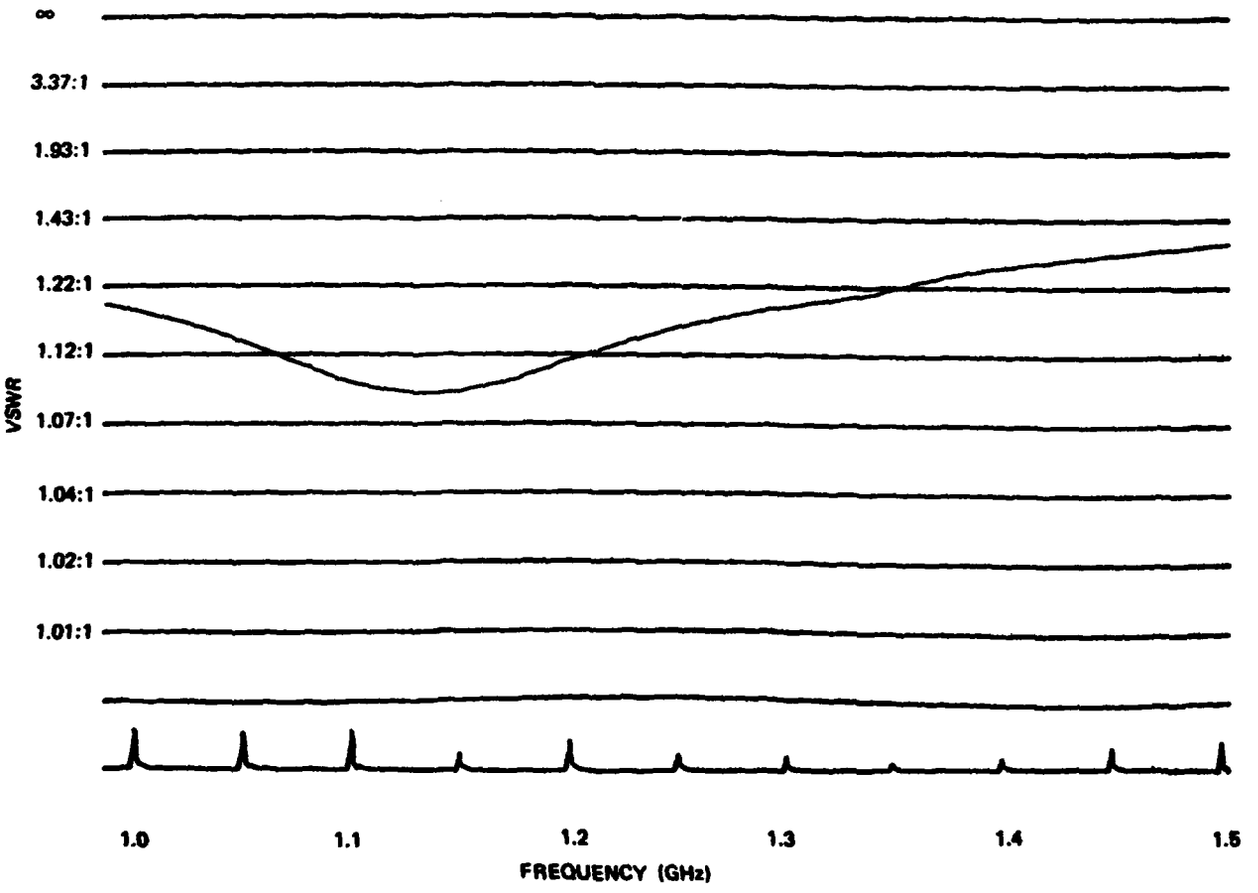

Figure 5-16. Swept-Frequency VSWR of Typical Flanged 50-Ohm Load Measured in Stripline Test Circuit

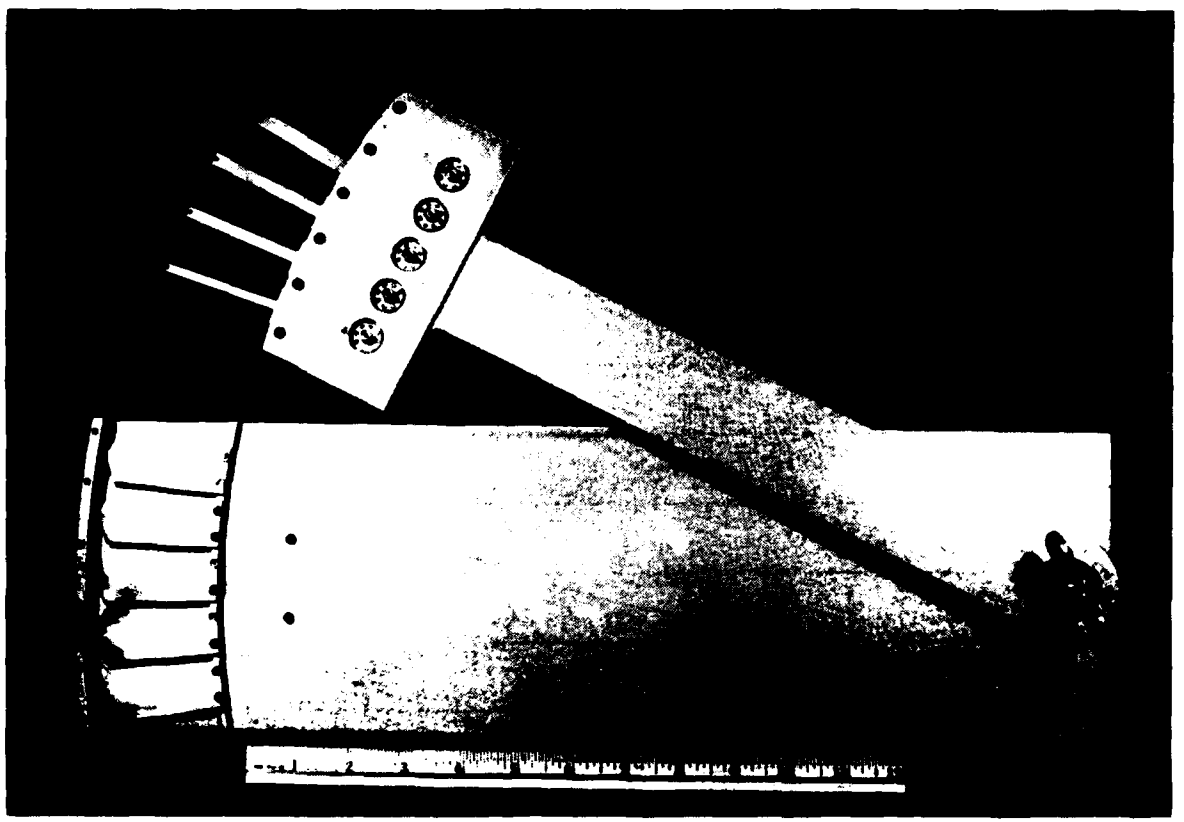

Figure 5-17. First Loop-Coupler Test Fixture

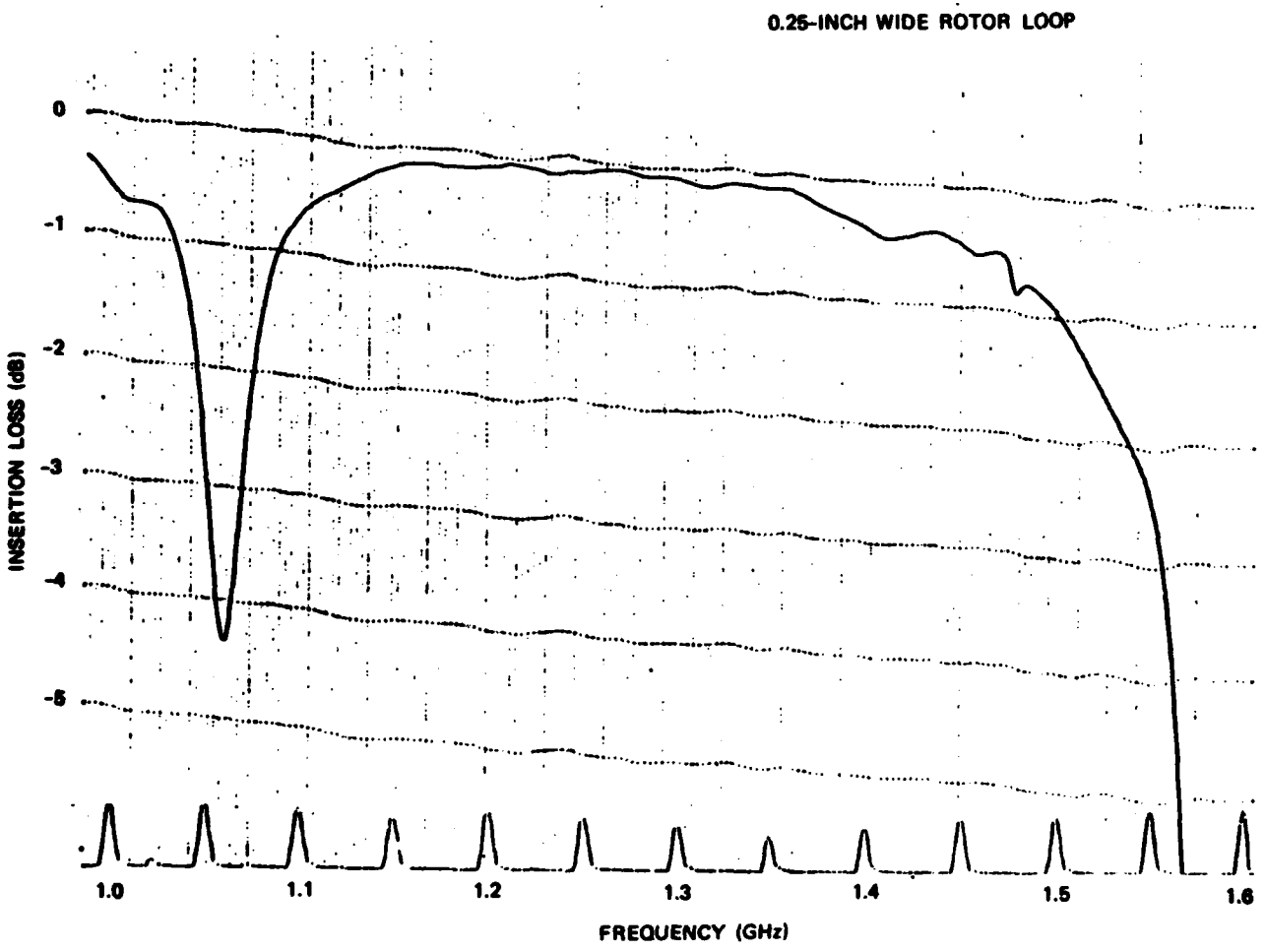

Figure 5-18. Swept-Frequency Insertion Loss of First Loop-Coupler Test Fixture

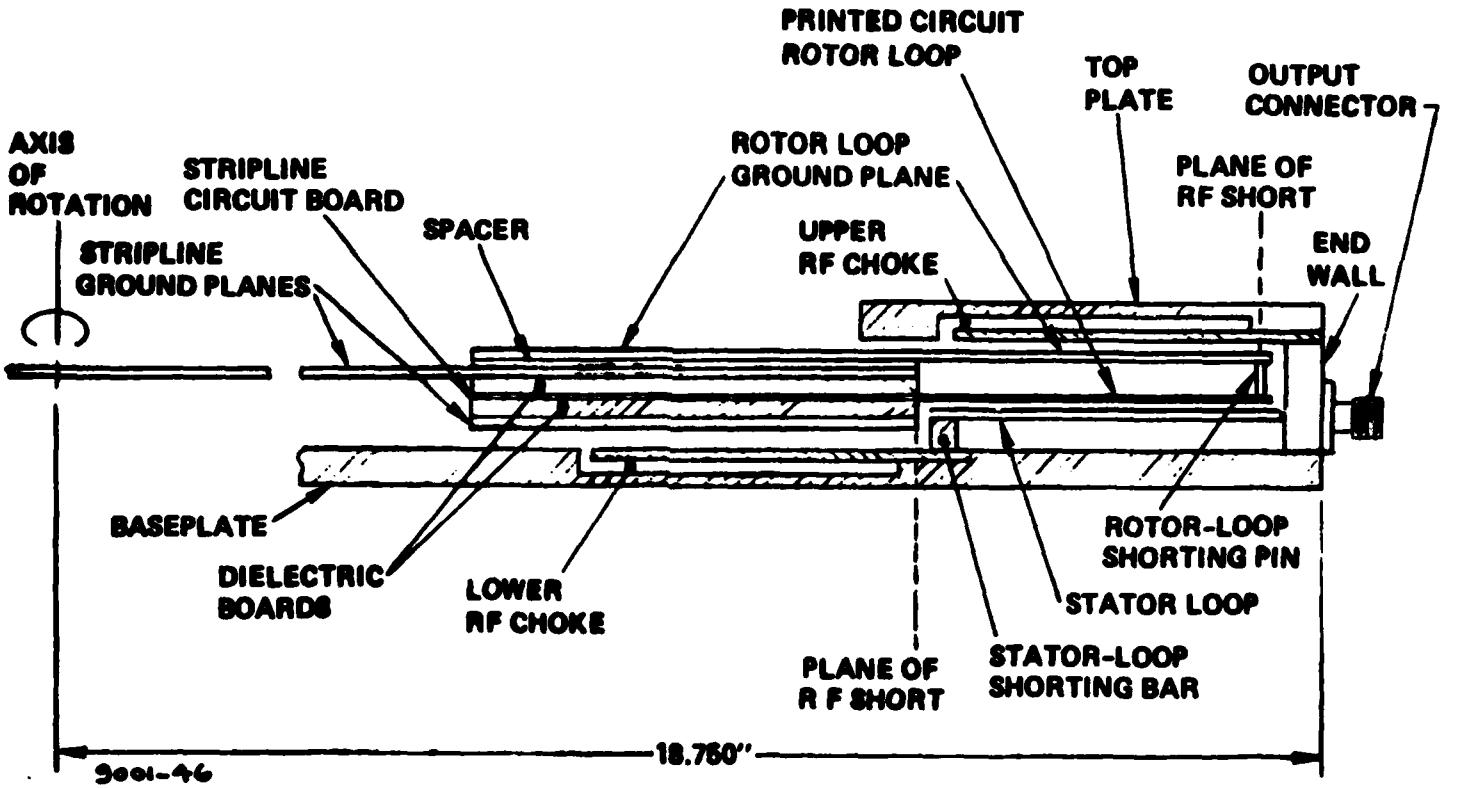

Figure 5-19. Cross Section of Loop-Coupler Test Section

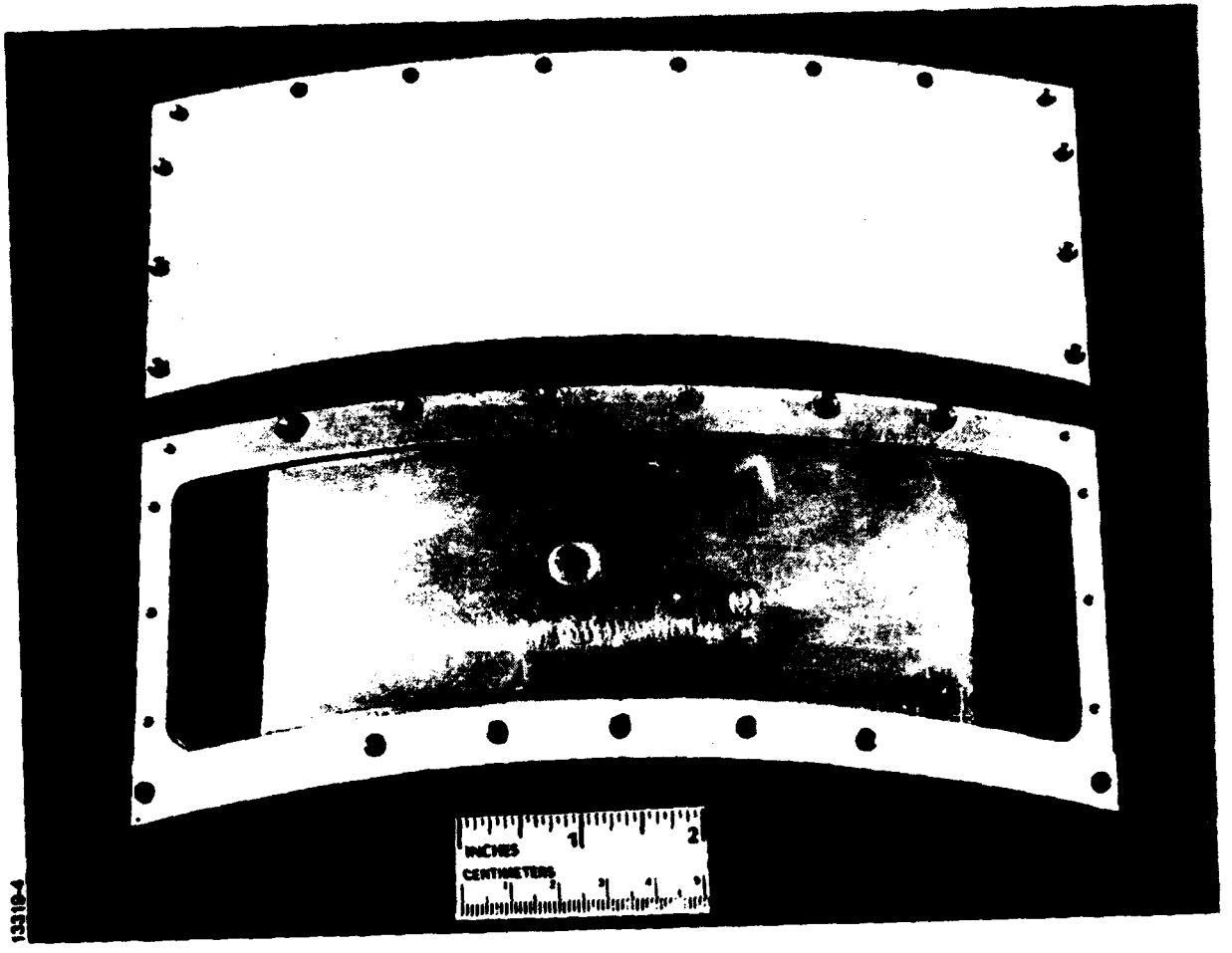

Figure 5-20. Upper RF Choke with Cover Plate Removed

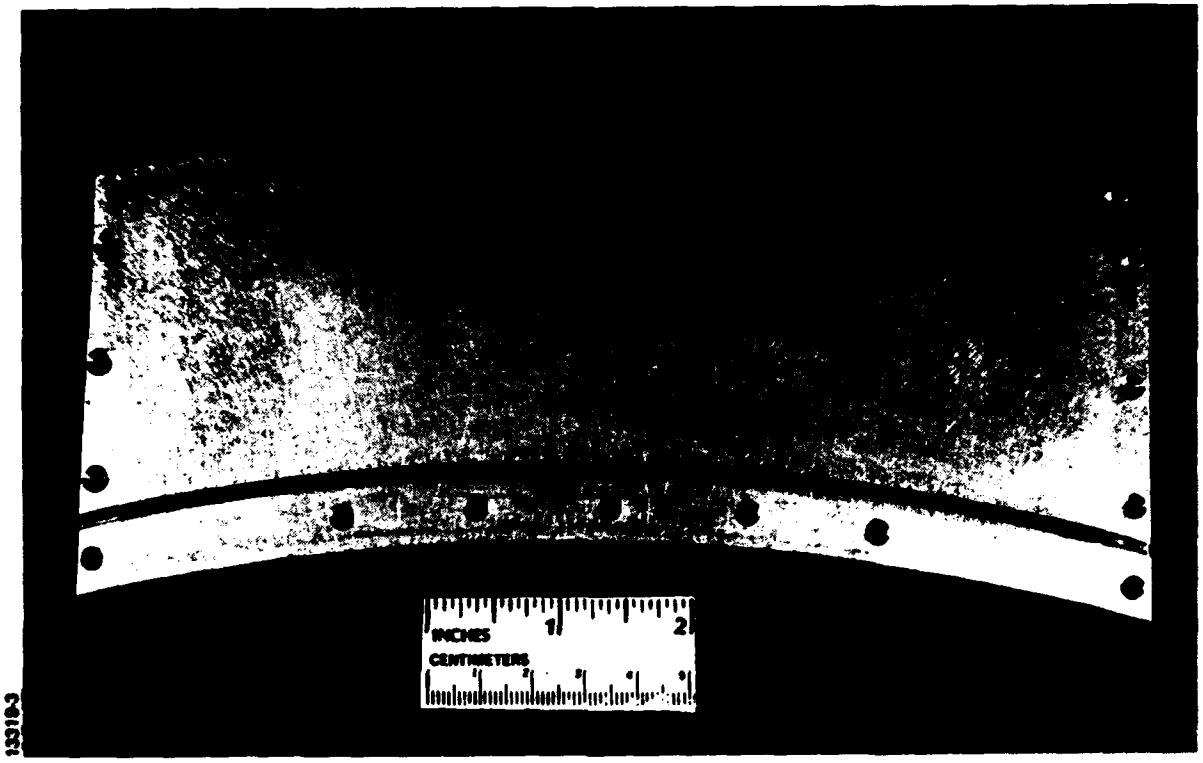

Figure 5-21. Upper RF Choke Assembled

Figure 5-22. Baseplate with Stator Loops and Lower RF Choke

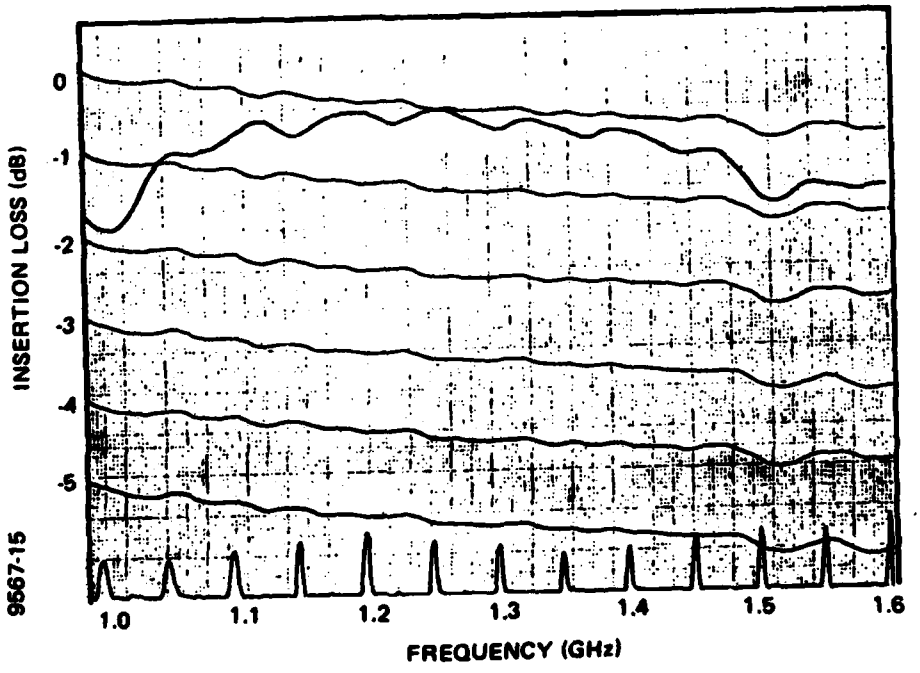

Figure 5-23. Measured Insertion Loss vs Frequency of Second Loop-Coupler Test Fixture

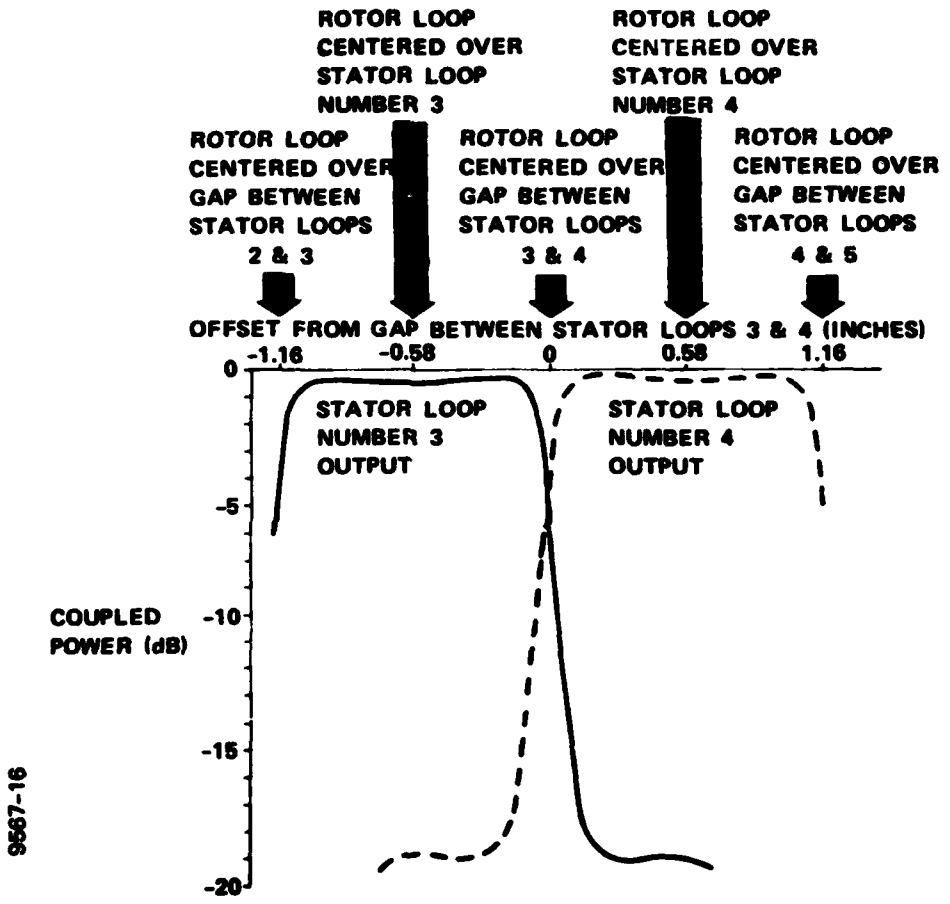

Figure 5-24. Measured Loop-Coupled Power vs Offset

SECTION 6

INTERIM FINDINGS AND CONCLUSIONS

Although the commutator feed assembly has not yet been built and evaluated, some reasonable predictions of performance can be made based on the results derived from various test fixtures.

It appears that insertion loss will be about 1.2 dB, just slightly higher than the goal of 1.0 dB, primarily because the average pathlength in stripline is appreciable: about 60 inches. Furthermore, insertion loss in the prototype model may run as high as 1.5 dB at 1.4 GHz, due to higher loss in the annular rotary coupler at that frequency. As noted previously, the annular rotary coupler used is a modified TACAN-band unit, and is not quite optimized for the 1.2 to 1.4 GHz band.

Input VSWR will be about 1.5:1, just slightly higher than the goal of 1.3:1. The input match can go as high as 2.0:1 at 1.4 GHz, once again because the annular rotary coupler is not optimized.

The performance of the commutator is quite broadband. The prototype unit will probably have reasonable performance from 1.0 to 1.6 GHz, and with further design, a 0.8 to 1.8 GHz unit appears to be feasible. The $\lambda/4$ overlap directional couplers, the delay line phase compensation, the non-contacting magnetic loop couplers, and the RF chokes are all inherently broadband devices. As noted before, the limiting item is the annular rotary coupler.

SECTION 7

WORK REMAINING

The revised commutator development schedule is shown in Figure 7-1.

Design of the stripline feed network, the loop couplers, and the annular RF chokes have been completed and finalized. The final mechanical layout is done, and the detail and assembly drawings are in process. Several of the detail parts are being fabricated. The two major purchased items are completed: the annular rotary coupler was received July 30th; the rotator pedestal assembly is ready for inspection, and due to be delivered August 17th.

Work that remains is completion of the detail and assembly drawings, fabrication of the stripline feed assembly and the stripline feed housing, and assembly and test of the completed commutator. The design effort is approximately 98 percent complete, and fabrication is about 10 percent done.

Delivery of the commutator to ESD, now scheduled for November 16th, has slipped about two months from the original mid-September date. The major reasons for the slippage are that the original schedule underestimated the lead time required to evaluate, select and purchase the copper-clad stripline laminate, and insufficient time was allowed for integrating the component parts (overlap directional couplers, delay lines, loads, matching networks, phase trimmers, rotor loops, etc.) into a large-scale stripline assembly.

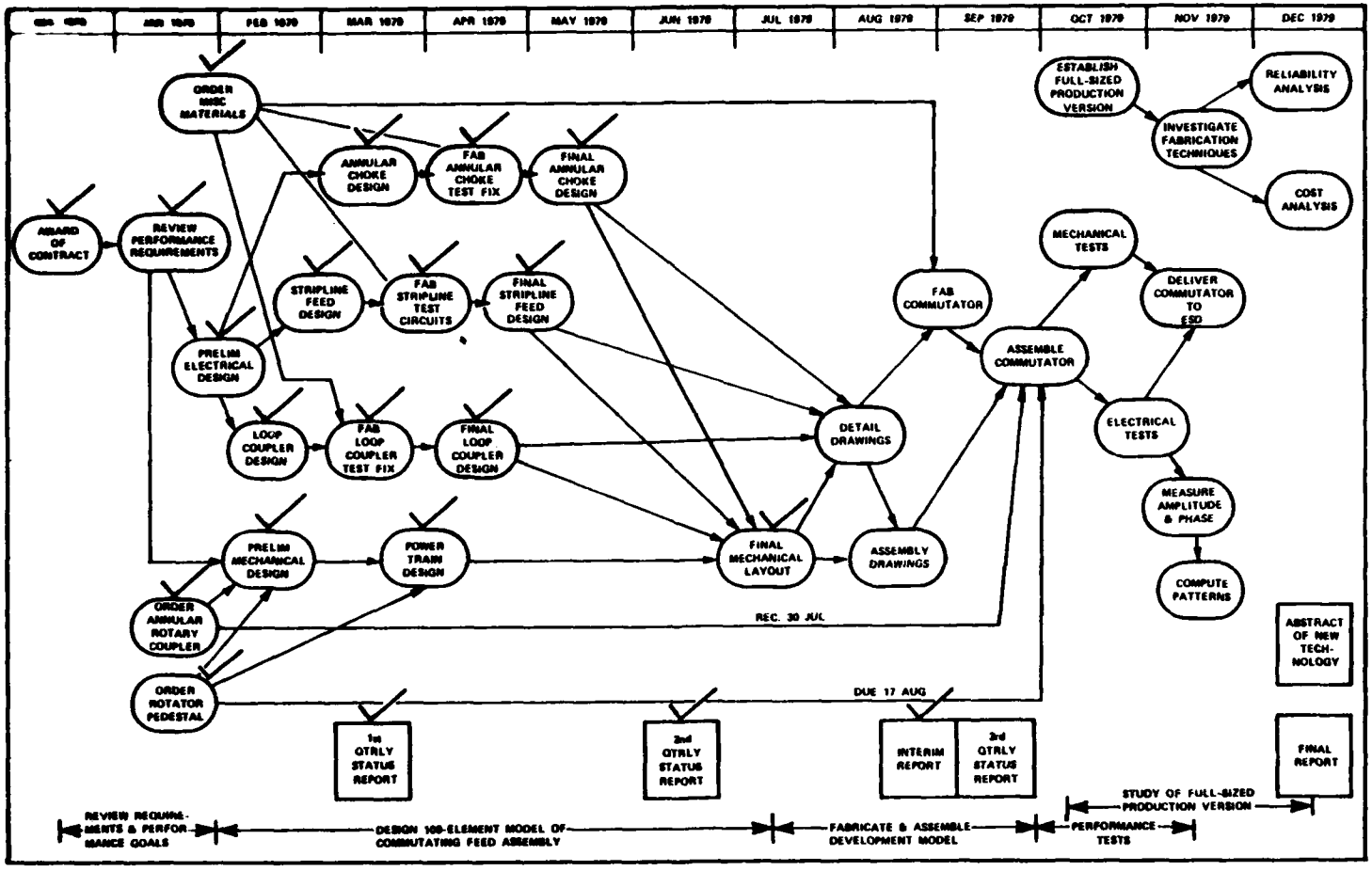

Figure 7-1. Revised Commutator Development Schedule

SECTION 8

PROGRAM PERSONNEL AND ORGANIZATION

The commutator development and study team are shown in Figure 8-1.

Mr. Wolfson, as Program Manager, has overall responsibility for budget, schedule and technical performance of this development. In addition, his technical contributions include the specification and vendor liaison of major purchased items, design of the loop-coupler test fixtures, and preparation of quarterly and technical reports.

Mr. Charlton proposed the design concept for the commutating feed assembly that is being developed on this program. He also did the antenna system analysis, the azimuth pattern computations, and the analytical design of the stripline feed network.

Mr. Fletcher provided background information on the UAR Program, plus valuable inputs concerning system performance.

Dr. Ching-Fai Cho is responsible for most of the development and evaluation of the stripline feed network and the loop couplers, as well as overall integration of the commutator.

Mr. Fernandez did the mechanical design, including preliminary drive-train analysis, selection of bearings, housing layout, support structure design, and liaison with drafting and model shop.

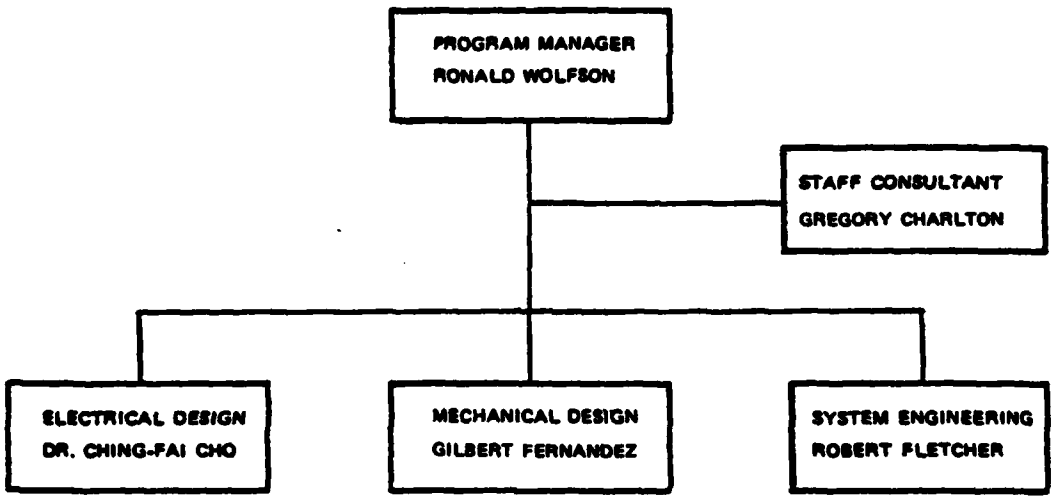

Figure 8-1. Commutator Development and Study Team